



The declining uptake rate of atmospheric CO₂ by land and ocean sinks

M. R. Raupach et al.

This discussion paper is/has been under review for the journal Biogeosciences (BG).
Please refer to the corresponding final paper in BG if available.

The declining uptake rate of atmospheric CO₂ by land and ocean sinks

M. R. Raupach^{1,2}, M. Gloor³, J. L. Sarmiento⁴, J. G. Canadell^{1,2}, T. L. Frölicher^{4,5},
T. Gasser^{6,7}, R. A. Houghton⁸, C. Le Quéré⁹, and C. M. Trudinger¹⁰

¹CSIRO, Centre for Australian Weather and Climate Research, Canberra, ACT 2601, Australia

²Global Carbon Project, CSIRO Marine and Atmospheric Research, Canberra, ACT 2601, Australia

³School of Geography, University of Leeds, Woodhouse Lane LS9 2JT, UK

⁴Program in Atmospheric and Oceanic Sciences, Princeton University, Sayre Hall, Forrestal Campus, Princeton, NJ 08540-6654, USA

⁵Environmental Physics, Institute of Biogeochemistry and Pollutant Dynamics, ETH Zürich, Switzerland

⁶Centre International de Recherche en Environnement et Développement, CNRS-CIRAD-EHESS-AgroParisTech-PontsParisTech, Campus du Jardin Tropical, 94736 Nogent-sur-Marne Cedex, France

⁷Laboratoire des Sciences du Climat et de l'Environnement, CEA-CNRS-UVSQ, CE l'Orme des Merisiers, 91191 Gif-sur-Yvette Cedex, France

⁸Woods Hole Research Center, Falmouth, Massachusetts 02540, USA

⁹Tyndall Centre for Climate Change Research, University of East Anglia, Norwich NR4 7TJ, UK

Title Page

Abstract

Introduction

Conclusions

References

Tables

Figures



Back

Close

Full Screen / Esc

Printer-friendly Version

Interactive Discussion

¹⁰CSIRO, Centre for Australian Weather and Climate Research, Aspendale, Victoria 3195, Australia

Received: 26 October 2013 – Accepted: 30 October 2013 – Published: 27 November 2013

Correspondence to: M. R. Raupach (michael.raupach@csiro.au)

Published by Copernicus Publications on behalf of the European Geosciences Union.

BGD

10, 18407–18454, 2013

The declining uptake rate of atmospheric CO₂ by land and ocean sinks

M. R. Raupach et al.

Title Page

Abstract

Introduction

Conclusions

References

Tables

Figures



Back

Close

Full Screen / Esc

Printer-friendly Version

Interactive Discussion



Abstract

Through 1959–2012, an airborne fraction (AF) of 44 % of total anthropogenic CO₂ emissions remained in the atmosphere, with the rest being taken up by land and ocean CO₂ sinks. Understanding of this uptake is critical because it greatly alleviates the emissions reductions required for climate mitigation. An observable quantity that reflects sink properties more directly than the AF is the CO₂ sink rate (k_S), the combined land-ocean CO₂ sink flux per unit excess atmospheric CO₂ above preindustrial levels. Here we show from observations that k_S declined over 1959–2012 by a factor of about 1/3, implying that CO₂ sinks increased more slowly than excess CO₂. We attribute the decline in k_S to four mechanisms: slower-than-exponential CO₂ emissions growth (~ 35 % of the trend), volcanic eruptions (~ 25 %), sink responses to climate change (~ 20 %), and nonlinear responses to increasing CO₂, mainly oceanic (~ 20 %). The first of these mechanisms is associated purely with extrinsic forcings, and the last two with intrinsic, nonlinear responses of sink processes to changes in climate and atmospheric CO₂. Our results indicate that the effects of these intrinsic, nonlinear responses are already detectable in the global carbon cycle. Although continuing future decreases in k_S will occur under all plausible CO₂ emission scenarios, the rate of decline varies between scenarios in non-intuitive ways because extrinsic and intrinsic mechanisms respond in opposite ways to changes in emissions: extrinsic mechanisms cause k_S to decline more strongly with increasing mitigation, while intrinsic mechanisms cause k_S to decline more strongly under high-emission, low-mitigation scenarios as the carbon-climate system is perturbed further from a near-linear regime.

1 Introduction

The properties of natural land and ocean CO₂ sinks have major implications for climate mitigation goals. The CO₂ airborne fraction (AF, the fraction of total anthropogenic CO₂ emissions from fossil fuels and net land use change that accumulates in the at-

BGD

10, 18407–18454, 2013

The declining uptake rate of atmospheric CO₂ by land and ocean sinks

M. R. Raupach et al.

Title Page

Abstract

Introduction

Conclusions

References

Tables

Figures

⏪

⏩

◀

▶

Back

Close

Full Screen / Esc

Printer-friendly Version

Interactive Discussion



mosphere; see Table 1) determines the fraction of emissions that contribute to rising atmospheric CO₂ concentrations, with the remainder (the sink fraction, SF = 1 – AF) being absorbed by land and ocean sinks. Changes in the AF and SF therefore affect the mitigation challenge.

5 The AF has been nearly constant on average since 1958 (the commencement of high-quality atmospheric CO₂ measurements) at a mean of about 0.44 (Ballantyne et al., 2012; Canadell et al., 2007; Knorr, 2009; Le Quéré et al., 2009; Tans, 2009), with significant interannual variability (Keeling and Revelle, 1985). Some analyses (Canadell et al., 2007; Le Quéré et al., 2009) have detected a small increasing trend in the AF since 1958 at a mean relative growth rate of about 0.2 % yr⁻¹, with significance (probability of positive trend) in the range 0.8 to 0.9. Methodological issues have been raised to question this result, concerning trend detection methods (Knorr, 2009), data (Ballantyne et al., 2012; Francey et al., 2010) and uncertainty analyses (Ballantyne et al., 2012). Nevertheless, multiple studies find results for the magnitude and significance of the AF trend that are in approximate agreement when consistent definitions are used (Ballantyne et al., 2012; Canadell et al., 2007; Knorr, 2009; Le Quéré et al., 2009).

20 The AF and its trend do not provide clear information about the behaviour or “efficiency” of CO₂ sinks, for two reasons. First, the AF mixes information about sinks and anthropogenic emissions. It has long been known that a constant or zero-trend AF would be expected under a “LinExp” idealisation of the carbon cycle, in which land and ocean CO₂ sinks increase linearly with excess CO₂ above preindustrial concentrations (assumption “Lin”) and total anthropogenic CO₂ emissions increase exponentially (“Exp”) (Bacastow and Keeling, 1979; Gloor et al., 2010; Hofmann et al., 2009; Raupach, 2013; Tans, 2009). Therefore, even when sinks are linear in excess CO₂, an AF trend appears when emissions increase non-exponentially. Second, the AF trend is strongly influenced by natural variability from major volcanic eruptions (Frölicher et al., 2013; Sarmiento et al., 2010) – a non-anthropogenic external influence – and inter-

The declining uptake rate of atmospheric CO₂ by land and ocean sinks

M. R. Raupach et al.

Title Page

Abstract

Introduction

Conclusions

References

Tables

Figures



Back

Close

Full Screen / Esc

Printer-friendly Version

Interactive Discussion



annual climate variability, predominantly El Niño–Southern Oscillation (ENSO) (Keeling and Revelle, 1985).

Recognising these issues with the interpretation of the AF, we here provide a new diagnosis and attribution of CO₂ sink behaviour using a different diagnostic, the CO₂ sink rate.

2 The CO₂ sink rate

The CO₂ uptake rate by land and ocean sinks ($k_S = f_{IS}/c_A$, henceforth the CO₂ sink rate) is the combined land-ocean CO₂ sink flux (f_{IS}) per unit mass of excess atmospheric CO₂ above preindustrial concentrations (c_A). It has dimension 1/time.

The main properties of k_S are as follows. First, a simple physical interpretation is that k_S is the instantaneous fractional rate of decrease in excess CO₂ due to sinks, or the “sink efficiency” (Gloor et al., 2010). Second, a trend in k_S indicates a difference in the relative growth rates of sinks and excess CO₂ (Table 2). Third, k_S (unlike the AF) can be split into additive components for land and ocean sinks (Table 1), or their regional sub-components (Raupach, 2013). Fourth, k_S depends directly on the sink flux and only indirectly on emissions trajectories through their effect on excess CO₂, whereas the AF is directly affected as much by a change in emissions as a change in sinks (Gloor et al., 2010). Therefore k_S is a stronger and more appropriate diagnostic for sink properties than the AF.

Fifth, k_S constitutes an observable weighted mean of the multiple time scales governing the global carbon cycle, describing their composite effect at any one time on excess atmospheric CO₂. It is well known that there is no single lifetime for atmospheric CO₂, because the carbon cycle includes multiple processes with time scales from days to millennia (Archer et al., 2009). The main processes are incorporated in all carbon cycle models. A linearised, multi-pool carbon cycle model is equivalent to a pulse response function for atmospheric CO₂ (the airborne fraction after time t of a pulse of CO₂ into the atmosphere) of the form of a sum of exponentials: $G(t) = \sum a_m \exp(-\lambda_m t)$,

The declining uptake rate of atmospheric CO₂ by land and ocean sinks

M. R. Raupach et al.

Title Page

Abstract

Introduction

Conclusions

References

Tables

Figures

⏪

⏩

◀

▶

Back

Close

Full Screen / Esc

Printer-friendly Version

Interactive Discussion



where the sum is over a set of modes m with turnover rates λ_m and weights a_m (Joos et al., 2013). The modes are a set of independent carbon pools $z_m(t)$, superpositions of physical carbon pools, that sum to the atmospheric excess carbon $c_A(t)$ (Raupach, 2013). It can be shown (see Appendix A) that

$$k_S = \sum_m b_m \lambda_m \quad (1)$$

where $b_m (= z_m/c_A)$ is the fraction of c_A in mode m , summing over m to 1. Thus, k_S is a weighted sum of the turnover rates λ_m . The weights b_m are time-dependent in linearised, pulse-response-function models of the carbon cycle, and the rates λ_m are also time-dependent in nonlinear models. Hence k_S depends on time through both b_m and λ_m . Equation (1) shows how k_S aggregates the effects of multiple processes with different rates to determine the net drawdown rate of atmospheric CO₂ by sinks at any particular time.

Sixth, under the LinExp idealisation defined above, both k_S and the AF are constant in time (Raupach, 2013). Conversely, neither k_S nor the AF are constant if CO₂ sinks are nonlinear in excess CO₂ (departure from “Lin”) or emissions are non-exponential (departure from “Exp”).

Seventh, the significance of k_S is enhanced by the fact that it can be readily measured (like the AF) from basic data on global CO₂ emissions and concentrations (Table 1). Observed variations in k_S are analysed here to identify underlying drivers of changes in carbon sinks.

3 Estimation of trends

Monthly trajectories for AF and k_S from January 1959 to December 2012 (henceforth 1959.0–2013.0) are shown in Fig. 1. These were obtained from collated data (Le Quéré et al., 2013) on CO₂ emissions from fossil fuels (f_{Fossil}) and net land use change (f_{LUC}), together with global atmospheric CO₂ concentrations; see Appendix B for details and

18412

BGD

10, 18407–18454, 2013

The declining uptake rate of atmospheric CO₂ by land and ocean sinks

M. R. Raupach et al.

Title Page

Abstract

Introduction

Conclusions

References

Tables

Figures

⏪

⏩

◀

▶

Back

Close

Full Screen / Esc

Printer-friendly Version

Interactive Discussion



references to primary sources. To quantify trends in AF and k_S we used several different data treatments (Appendix C) and trend estimation methods (Appendix D). Our measure of trend is the relative growth rate (RGR), with dimension 1/time, defined for a series $X(t)$ as $RGR(X) = \langle d(\ln X)/dt \rangle \approx \langle X \rangle^{-1} \langle dX/dt \rangle$, where angle brackets denote expected values (Appendix E).

For AF, our best trend estimate (Fig. 2 and Table 3) is $RGR(AF) = 0.27 \pm 0.20 \text{ \%yr}^{-1}$ ($\pm 1\sigma$, $P = 0.91$) about a mean $\langle AF \rangle$ of 0.44 over 1959.0–2013.0, where $\pm 1\sigma$ denotes a 1 standard deviation confidence interval, and the significance (P) is the probability of positive trend. Both the trend and its significance are comparable with earlier studies cited in the Introduction, when consistent definitions are used; in particular, the statistical significance of the AF trend is found by all studies (including this one) to be less than 95 %, between “likely” and “very likely” in the standard terminology of the Intergovernmental Panel on Climate Change (IPCC, 2007).

For k_S , the best trend estimate (Fig. 2 and Table 4) is $RGR(k_S) = -0.93 \pm 0.17 \text{ \%yr}^{-1}$ ($\pm 1\sigma$, $P > 0.999$ for negative trend), about a mean $\langle k_S \rangle$ of 0.028 ($= 1/36$) yr^{-1} . The observed decreasing trend in k_S is statistically robust and “virtually certain” in IPCC terminology, in contrast with the AF trend.

The above uncertainty estimates for trends in AF and k_S reflect variability associated with CO_2 growth rate, but not uncertainties in CO_2 emissions from fossil fuels (f_{Fossil}) and net land use change (f_{LUC}). As described in detail in Appendix F, these uncertainties were assessed by repeating the estimation of $RGR(AF)$ and $RGR(k_S)$ with three alternative f_{Fossil} trajectories (Francey et al., 2010; Gregg et al., 2008; Guan et al., 2012) (Fig. F1) and eleven alternative f_{LUC} trajectories (Le Quéré et al., 2009) (Fig. F3). The resulting trend estimates are statistically indistinguishable from our best estimates (Appendix F).

BGD

10, 18407–18454, 2013

The declining uptake rate of atmospheric CO_2 by land and ocean sinks

M. R. Raupach et al.

Title Page

Abstract

Introduction

Conclusions

References

Tables

Figures

⏪

⏩

◀

▶

Back

Close

Full Screen / Esc

Printer-friendly Version

Interactive Discussion

4 Attribution of trends

Attribution of an observed effect from multiple processes to individual process contributions is necessarily a modelling exercise, with results that are model-dependent and not directly verifiable by observations (UNFCCC, 2002). Here we attribute trends in AF and k_S by using a nonlinear carbon–climate model that approximately reproduces observed trends in AF and k_S in its full form. By progressively simplifying the model to eventually reach the LinExp idealisation in which all trends are zero, the contributions of different factors to observed trends can be identified.

The model is the Simple Carbon–Climate Model (SCCM), a globally aggregated model of the carbon–climate system (Harman et al., 2011; Raupach, 2013; Raupach et al., 2011). Model state variables comprise one atmospheric CO₂ store, two land carbon stores, four perturbation carbon stores in the ocean, the atmospheric concentrations of four major non-CO₂ greenhouse gases (CH₄, N₂O and two representative halocarbons), and three perturbation global temperatures representing heat stores with different turnover rates (Li and Jarvis, 2009). Carbon in the ocean mixed layer is modelled using a pulse response function that emulates the mixing dynamics of several complex ocean circulation models (Joos et al., 1996). The model ocean–atmosphere CO₂ flux incorporates full, nonlinear ocean carbonate chemistry (Lewis and Wallace, 1998). The model terrestrial biosphere includes nonlinear dependences of terrestrial Net Primary Production (NPP) on CO₂ concentration and of heterotrophic respiration on temperature. The effect of volcanic activity on the terrestrial carbon cycle (Jones and Cox, 2001) is included through an enhancement factor for terrestrial NPP that is proportional to a global volcanic aerosol index (Ammann et al., 2003), tested using recent major eruptions. An important aspect for this work is that SCCM can be linearised analytically (Raupach, 2013), allowing linearisation to be included explicitly as a simplifying step. SCCM does not resolve interannual variability associated with short-term climate fluctuations, regionally specific processes, and climate effects on the carbon cycle beyond those captured by a response to global temperature.

BGD

10, 18407–18454, 2013

The declining uptake rate of atmospheric CO₂ by land and ocean sinks

M. R. Raupach et al.

Title Page

Abstract

Introduction

Conclusions

References

Tables

Figures

⏪

⏩

◀

▶

Back

Close

Full Screen / Esc

Printer-friendly Version

Interactive Discussion

The declining uptake rate of atmospheric CO₂ by land and ocean sinks

M. R. Raupach et al.

[Title Page](#)

[Abstract](#)

[Introduction](#)

[Conclusions](#)

[References](#)

[Tables](#)

[Figures](#)

[⏪](#)

[⏩](#)

[◀](#)

[▶](#)

[Back](#)

[Close](#)

[Full Screen / Esc](#)

[Printer-friendly Version](#)

[Interactive Discussion](#)



In Fig. 3, the comparison between the black (data) and red (full model) bars demonstrates that SCCM satisfactorily reproduces the observed trends in AF and k_S over 1959.0–2013.0. By contrast, most carbon–climate models in the C4MIP intercomparison (Friedlingstein et al., 2006) predict a negative AF trend over this period, of opposite sign to the observed positive trend, and also greatly underestimate the magnitude of the observed negative trend in k_S (see Appendix G for details). Tests of SCCM against observed time series of CO₂, temperature, AF and k_S (Figs. 4 and 5) also demonstrate satisfactory performance over this period. The model reproduces the observed perturbations in AF and k_S due to major volcanic eruptions (Fig. 5), but does not reproduce interannual climate variability.

Figure 3 shows the effects on the trends in AF and k_S of successively removing processes from the model, while leaving all model parameters unchanged. The first simplification (V1 to V2) is linearisation of the model carbon cycle, using the tangent-linear form of SCCM. This removes all nonlinear dependences of CO₂ fluxes and radiative forcing on carbon stores and temperatures, but retains linearised interactions among these quantities. The result is a reduction in the magnitude of the k_S trend by $\sim 20\%$ (noting that $RGR(k_S)$ is negative), most of the reduction being due to removal of nonlinearities associated with the dependence of ocean–air CO₂ exchange on atmospheric CO₂. The next simplification (V2 to V3) is carbon–climate decoupling, by removing all dependences of CO₂ fluxes on temperature through terrestrial NPP, heterotrophic respiration and ocean chemistry (consequently also removing effects of non-CO₂ gases on the carbon cycle). This reduces the magnitude of the k_S trend by another $\sim 20\%$ of its full-model value. Removal of the effects of volcanism on terrestrial NPP (V3 to V4) causes another $\sim 25\%$ reduction. The last $\sim 35\%$ of the k_S trend is removed by replacement of real total CO₂ emissions ($f_{\text{FOSS}} + f_{\text{LUC}}$), which depart from exponential growth (Gloor et al., 2010; Raupach, 2013), by an exponential trajectory with the same mean growth rate over 1850–2011 (V4 to V5). After all four simplification steps, the k_S trend is reduced to zero in the model, consistent with the theoretical requirement of the LinExp idealisation (Raupach, 2013).

We have repeated this progressive model simplification experiment with different orderings for process removal, finding that the above result is independent of ordering.

Not surprisingly, model simplification progressively weakens the agreement between model and observations as processes are removed (Figs. 6 and 7).

5 The sequence of effects of progressive model simplification is not as simple for AF as for k_S (Fig. 3). For AF, the largest single change is brought about by removal of volcanic effects: this eliminates the observed positive trend in AF, in accord with other findings (Frölicher et al., 2013). The proportional effects of the four simplification steps are not the same for the AF as for k_S because of constraining relationships between
10 their growth rates (Table 2).

5 Conclusions

The implications of this work can be summarised as follows. First, the trajectories of AF and k_S provide different insights into the behaviour of the carbon cycle. Trends in the AF indicate differences in the relative growth rates of excess CO_2 accumulation and anthropogenic CO_2 emissions, while trends in k_S indicate differences in the relative
15 growth rates of sinks and excess CO_2 concentration (Table 2). Immediate implications of the observed decline in k_S over 1959.0–2013.0 are that CO_2 sinks increased more slowly than excess CO_2 , and that the sink efficiency (the fractional rate of decrease in excess CO_2 due to sinks) decreased.

20 Second, the observed decline in k_S is projected to continue under all realistic emissions scenarios (Fig. 5). In contrast, future trends in AF are much more strongly dependent on emissions scenarios, with the AF becoming negative under strong-mitigation scenarios.

25 Third, k_S constitutes an observable weighted mean of the multiple rates λ_m of processes controlling the global carbon cycle, describing their combined effect on excess atmospheric CO_2 through land and ocean sinks. Over 1959.0–2013.0, the composite drawdown time scale $1/k_S$ increased from ~ 30 to ~ 45 yr, and is projected to increase

The declining uptake rate of atmospheric CO_2 by land and ocean sinks

M. R. Raupach et al.

Title Page

Abstract

Introduction

Conclusions

References

Tables

Figures



Back

Close

Full Screen / Esc

Printer-friendly Version

Interactive Discussion



further in future. Therefore the mix of carbon-cycle time scales contributing to draw-down of CO₂ by sinks has shifted observably towards longer scales, a trend that is projected to continue in future.

Fourth, we attribute the decline in k_S to four mechanisms. One of these – departure of emissions from exponential growth – is “extrinsic”, arising from external anthropogenic forcing of the carbon–climate system. Two others – nonlinear carbon cycle responses to CO₂ and carbon–climate coupling – are “intrinsic”, arising from process feedbacks in the system. Volcanic effects are both extrinsic and intrinsic, involving feedbacks triggered by non-anthropogenic forcing through aerosols. The primary extrinsic mechanism operates thus: when CO₂ emissions increase more slowly than exponentially, the fast-response, low-capacity modes of the carbon cycle saturate more rapidly than slow modes, so the weights b_m in Eq. (1) decrease with time for faster modes and increase for slower modes, causing k_S to decrease. These sink-capacity effects can be described by linear theory (Raupach, 2013). In contrast, the primary intrinsic mechanisms arise from nonlinear feedbacks that have the net effect of decreasing the turnover rates λ_m in Eq. (1), thence decreasing k_S . Respectively, the main (extrinsic intrinsic) mechanisms are essentially (linear, nonlinear) and act through (b_m , λ_m).

Fifth, the future rate of decline in k_S varies among emissions scenarios (Fig. 5). Extrinsic and intrinsic mechanisms respond in opposite ways to changes in emissions: extrinsic mechanisms cause k_S to decline more strongly with increasing mitigation, as emissions trajectories fall progressively further below exponential growth (for example, k_S would decrease very rapidly if anthropogenic CO₂ emissions were to stop instantly). In contrast, intrinsic mechanisms cause k_S to decline more strongly under high-emission, low-mitigation scenarios as the carbon–climate system is perturbed further from a near-linear regime and rates for individual sink processes decrease. The net result of these opposing influences is that projected future values of the composite drawdown time scale $1/k_S$ range from ~ 120 to ~ 180 yr (in 2100) for scenarios from emissions-intensive to strong-mitigation (Fig. 5).

BGD

10, 18407–18454, 2013

The declining uptake rate of atmospheric CO₂ by land and ocean sinks

M. R. Raupach et al.

Title Page

Abstract

Introduction

Conclusions

References

Tables

Figures

⏪

⏩

◀

▶

Back

Close

Full Screen / Esc

Printer-friendly Version

Interactive Discussion

The declining uptake rate of atmospheric CO₂ by land and ocean sinks

M. R. Raupach et al.

[Title Page](#)

[Abstract](#)

[Introduction](#)

[Conclusions](#)

[References](#)

[Tables](#)

[Figures](#)

[⏪](#)

[⏩](#)

[◀](#)

[▶](#)

[Back](#)

[Close](#)

[Full Screen / Esc](#)

[Printer-friendly Version](#)

[Interactive Discussion](#)

Sixth, the effects of intrinsic, nonlinear mechanisms (carbon-cycle responses to CO₂ and carbon–climate coupling) are already evident in the carbon cycle, together accounting for ~ 40 % of the observed decline in k_S over 1959.0–2013.0. These intrinsic mechanisms encapsulate the vulnerability of the carbon cycle to nonlinear system

5 feedbacks. By comparison, the extrinsic, sink-capacity mechanisms are much easier to describe. An important open question is how rapidly the intrinsic mechanisms and associated feedbacks will contribute to further decline in k_S under various emission scenarios.

Seventh, the approach of progressive model simplification used here can be applied to attribute trends in k_S with other suitable models. While our attribution is necessarily

10 restricted to processes resolved in the model used here, a more complex model could attribute trends to more finely resolved processes such as regional contributions to land and ocean sinks (Ciais et al., 2013). The approach ensures that all contributions sum to the full model trend in k_S . Such an attribution would show not only how different regions are contributing to the environmental service provided by land and ocean carbon sinks, as quantified by their additive contributions to the global sink flux or global sink rate k_S , but also how these contributions are changing in different ways in response to both

15 extrinsic (forcing) and intrinsic (feedback) influences.

Appendix A

20 Sink rate k_S as a weighted mean of turnover rates

Here it is shown that the sink rate k_S is a weighted mean of the turnover rates contributing to a pulse response function for atmospheric CO₂, following previous work (Raupach, 2013) with simplified notation.

At a high level of generality, a linearised, multi-pool model of the carbon cycle is

$$\frac{dc_i}{dt} = f_i(t) - \sum_j \mathbf{K}_{ij} c_j(t); \quad c_i(0) = 0 \quad (\text{A1})$$

where $c_i(t)$ is the excess carbon (the perturbation above a preindustrial equilibrium state) in pool i , $f_i(t)$ is the anthropogenic carbon input into pool i , and \mathbf{K}_{ij} is a transfer matrix describing inter-pool transfers. This is a coupled dynamical system that can be solved readily by method of normal modes. The approach is to transform the system to a new frame where the state variables $c_i(t)$ become “normal modes” satisfying independent, uncoupled equations. In this new frame, the atmospheric excess carbon pool c_A can be written as a sum of rescaled normal modes $z_m(t)$ (Raupach, 2013):

$$c_A(t) = \sum_m z_m(t) \quad (\text{A2})$$

The modes $z_m(t)$ are linear superpositions of the excess carbon pools $c_i(t)$, governed by

$$\frac{dz_m}{dt} = a_m f_E(t) - \lambda_m z_m; \quad z_m(0) = 0 \quad (\text{A3})$$

where λ_m is the turnover rate for mode m , and a_m is a weight (summing over m to 1) specifying the fraction of total emissions to the atmosphere ($f_E = f_{\text{FOSS}} + f_{\text{LUC}}$) entering mode m . The rates λ_m are the eigenvalues of the transfer matrix \mathbf{K}_{ij} . The solution for $c_A(t)$ is then given by

$$c_A(t) = \int_0^t G(t - \tau) f_E(\tau) d\tau \quad (\text{A4})$$

The declining uptake rate of atmospheric CO₂ by land and ocean sinks

M. R. Raupach et al.

Title Page

Abstract

Introduction

Conclusions

References

Tables

Figures

⏪

⏩

◀

▶

Back

Close

Full Screen / Esc

Printer-friendly Version

Interactive Discussion



where

$$G(t) = \sum_m a_m \exp(-\lambda_m t) \quad (\text{A5})$$

is a pulse response function (PRF) for atmospheric CO₂ (the fraction of an instantaneous pulse of CO₂ into the atmosphere that remains airborne after time t) taking the form of a sum of decaying exponential terms with decay rates λ_m . One of the decay rates is often taken as zero², so that $G(t) = a_0 + a_1 \exp(\lambda_1 t) + \dots$

Summing Eq. (A3) over modes m , the excess atmospheric CO₂ is governed by

$$\frac{dc_A}{dt} = f_E(t) - \sum_m \lambda_m z_m \quad (\text{A6})$$

From equations in Table 1, the atmospheric CO₂ budget (with the total CO₂ sink parameterised using the sink rate k_S) is:

$$\frac{dc_A}{dt} = f_E(t) - k_S c_A \quad (\text{A7})$$

Equating the last terms in Eqs. (A6) and (A7), it follows that

$$k_S = \sum_m b_m \lambda_m; \quad b_m = z_m / c_A \quad (\text{A8})$$

Hence k_S is a weighted mean of the turnover rates λ_m for different modes. The weights b_m are the fractions of c_A appearing in the modes m , and from Eq. (A2), these weights sum to 1.

The weights b_m depend on time in general, because the modes z_m grow at different rates λ_m . If emissions $f_E(t)$ were steady, z_m for faster modes with larger λ_m would saturate to the equilibrium value $f_{E(\text{steady})} / \lambda_m$ more rapidly than z_m for slower modes. This would cause b_m to give progressively higher relative weight to slower modes as time advances, so that k_S would decrease. In the case where emissions increase exponentially, k_S is constant in time, like the AF. An exponentially increasing trajectory $f_E(t)$ is the only case leading to constant k_S and AF (Raupach, 2013).

The declining uptake rate of atmospheric CO₂ by land and ocean sinks

M. R. Raupach et al.

Title Page

Abstract

Introduction

Conclusions

References

Tables

Figures

⏪

⏩

◀

▶

Back

Close

Full Screen / Esc

Printer-friendly Version

Interactive Discussion



Appendix B

Primary data sources

Primary data are as for the global CO₂ budget compiled by the Global Carbon Project to 2011 (Le Quéré et al., 2013), with extensions to 2012 based on primary data sources (Fig. B1). Details are:

Atmospheric CO₂ accumulation: the atmospheric CO₂ accumulation rate is $c'_A = dc_A/dt$ (in PgCy⁻¹) where $c_A = 2.127([\text{CO}_2] - [\text{CO}_2]_q)$ (Table 1). Three time series for monthly [CO₂] were used: in-situ [CO₂] at Mauna Loa (MLO, March 1958 onward), flask [CO₂] at the South Pole (SPO, June 1957 onward), and a globally averaged CO₂ series from multiple stations (GLB, January 1980 onward). MLO and SPO data were from the Scripps Institution of Oceanography (Keeling et al., 2005, 2001; Scripps-CO₂-Program, 2013); GLB data were from the Earth Systems Research Laboratory of the National Oceanographic and Atmospheric Administration (NOAA-ESRL, 2013). The series used here were gap-filled and deseasonalised by removal of annual cyclic components. Global mean [CO₂] from March 1958 to December 1979 was estimated as (MLO + SPO)/2, and from January 1980 to January 2011 by the GLB value. The monthly CO₂ growth rate (with annual cycle removed) was calculated from each series by a centred first difference.

CO₂ emissions: annual global data on CO₂ emissions from fossil fuels and other industrial processes (f_{FOSS}) are from the Carbon Dioxide Analysis and Information Center (CDIAC) at the Oak Ridge National Laboratory, USA (Boden et al., 2013). Data on CO₂ emissions from net land use change (f_{LUC}) are based on a bookkeeping method (Houghton, 2010). Cumulative fossil-fuel emissions ($Q_{\text{FOSS}}(t)$) were estimated by accumulating $f_{\text{FOSS}}(t)$ from 1751. Cumulative LUC emissions ($Q_{\text{LUC}}(t)$) were estimated by accumulating $f_{\text{LUC}}(t)$ from 1751, with backward linear extrapolation from the earliest year of data (1851) to zero in 1751.

The declining uptake rate of atmospheric CO₂ by land and ocean sinks

M. R. Raupach et al.

Title Page

Abstract

Introduction

Conclusions

References

Tables

Figures

⏪

⏩

◀

▶

Back

Close

Full Screen / Esc

Printer-friendly Version

Interactive Discussion



Appendix C

Data treatments

The five data treatments for time series of AF were as follows.

1. $AF(a)$ is a simple, untreated annual AF time series: $AF(a) = (\Delta c_A / \Delta t) / (f_{\text{Foss}} + f_{\text{LUC}})$ with $\Delta t = 1$ yr and discretisation to yield year-centered estimates (e.g. 2009.5); Δc_A is the increment in the atmospheric mass of CO_2 at successive year starts (e.g. 2009.0 to 2010.0), and emissions f_{Foss} and f_{LUC} are year-centred (e.g. 2009.5).
2. $AF(m)$ is a simple, untreated monthly AF time series: $AF(m) = (\Delta c_A / \Delta t) / (f_{\text{Foss}} + f_{\text{LUC}})$ with $\Delta t = 1$ month and discretisation to yield 12 month-centred estimates per year (at $2009 + 1/24, 2009 + 3/24, \dots, 2009 + 23/24$). Linear interpolation between annual data points was used to estimate emissions at intervening times, and linear interpolation between monthly data points was used similarly for concentrations.
3. $AF(m, s)$ is a version of the monthly series $AF(m)$ with 15 month running-mean smoothing applied to time series of dc_A/dt before calculation of the AF. This removes most high-frequency (faster than annual) variability (Raupach et al., 2008).
4. $AF(m, n)$ is a monthly AF series without smoothing but with noise reduction by removal of the fluctuating component linearly correlated with El-Niño-Southern-Oscillation (ENSO) and volcanic aerosol indices. These together account for about half the variance in dc_A/dt from fluctuations shorter than a decade (Raupach et al., 2008). Contributions to the other half of the variance include climate modes other than ENSO, nonlinear effects, and regionally specific effects.

BGD

10, 18407–18454, 2013

The declining uptake rate of atmospheric CO_2 by land and ocean sinks

M. R. Raupach et al.

Title Page

Abstract

Introduction

Conclusions

References

Tables

Figures

⏪

⏩

◀

▶

Back

Close

Full Screen / Esc

Printer-friendly Version

Interactive Discussion

5. $AF(m, s, n)$ is a monthly AF series with both 15 month smoothing as in $AF(m, s)$, and noise reduction as in $AF(m, n)$. Results are insensitive to the order in which smoothing and noise reduction are applied.

For the CO_2 sink rate k_S , similar data treatments were used. This yielded five series
5 $k_S(a)$, $k_S(m)$, $k_S(m, s)$, $k_S(m, n)$ and $k_S(m, s, n)$.

Appendix D

Trend estimation methods

The four trend estimation methods were as follows.

1. *Linear regression*: simple least-squares linear regression overestimates the confidence in the estimated trend, yielding a spuriously low CI (confidence interval) and spuriously high P value (probability of positive trend) when a series is temporally autocorrelated, as for all our series.
2. *Stochastic method*: this method estimates the confidence interval for the trend with account for the temporal autocorrelation of the time series (Canadell et al., 2007; Le Quéré et al., 2007). For a time series $X(t)$, steps are: (a) the trend X^T is found by conventional least-squares linear regression, yielding a trend line $X^T = x_0 + x_1 t$. (b) The lagged autocorrelation function of the residual $(X - X^T)$ is fitted with an autoregressive (AR) model (Box et al., 1994). (c) An ensemble of 1000 stochastic realisations of the data is generated with mean trend X^T and residuals correlated as in the AR model. Members of this ensemble have a similar mean trend and autocorrelation function to the original series, but vary stochastically among realisations. (d) The trend for each member of this ensemble is determined by least-squares linear regression, yielding 1000 estimates of the trend (x_1) . (e) The probability density function (PDF) of trend estimates x_1 is calculated,

The declining uptake rate of atmospheric CO_2 by land and ocean sinks

M. R. Raupach et al.

Title Page

Abstract

Introduction

Conclusions

References

Tables

Figures



Back

Close

Full Screen / Esc

Printer-friendly Version

Interactive Discussion



yielding trend statistics. The P value is the fraction of the 1000 estimates of x_1 that is greater than 0.

3. *Bootstrap method*: both regression and stochastic methods suffer from sensitivity to the choice of start and end times, yielding different results if start or end times are shifted by a few months. The bootstrap method overcomes this problem. An ensemble of time series is constructed by selecting continuous subseries from the original series $X(t)$ with randomised start and end times, subject to the condition that the minimum record length of each ensemble member is at least a fraction f_{Bts} of the complete record. The ensemble is constructed with replacement, so this is a “bootstrap” method. The members of the ensemble are not independent, but represent different possible realisations of the observational constraints determining the length of the series. The choice of f_{Bts} is a compromise between the requirements that (a) ensemble members include most of the original series, and (b) the variations in start and end times be enough to randomise their effects. The latter requirement demands that the omitted portions of the record typically encompass several integral time scales for the series $X(t)$. We used $f_{\text{Bts}} = 0.8$. The bootstrap method reduces the influence of the choice of start and end times and therefore yields an improved estimate of mean trend, but provides no estimate of uncertainty information (CI or P value) because the ensemble members are not independent.

4. *Combined method*: here both the stochastic and bootstrap methods are applied together. Steps are: (a) an ensemble of continuous subseries with randomised start and end times is selected as in the bootstrap method. (b) The trend (x_1) for each subseries is determined by linear regression. (c) The lagged autocorrelation function for the entire series is found, as in the stochastic method. (d) Using this autocorrelation function and the trend for each subseries, a stochastic ensemble of series is generated. (e) The trend for each ensemble member is found by linear regression. (f) Statistics of the ensemble of trend estimates are found as in the

The declining uptake rate of atmospheric CO₂ by land and ocean sinks

M. R. Raupach et al.

Title Page

Abstract

Introduction

Conclusions

References

Tables

Figures



Back

Close

Full Screen / Esc

Printer-friendly Version

Interactive Discussion



stochastic method. The combined method provides our best estimates, because it combines the benefits of the bootstrap method for estimation of trend and the stochastic method for confidence interval.

Appendix E

5 Relative growth rate

For a series $X(t)$ with all $X(t) > 0$, the relative growth rate is

$$\text{RGR}(X) = \left\langle \frac{d \ln X(t)}{dt} \right\rangle \quad (\text{E1})$$

where angle brackets denote expected values. This definition has the benefit that, when the expected value is evaluated as the regression slope of $\ln X$, identities for relative growth rates of products, powers and quotients (Table 2) are automatically satisfied.

Noisy series $X(t)$ often have values of both signs, for example, the monthly series $AF(m)$ and $k_S(m)$. In this case, Eq. (E1) must be approximated as

$$\text{RGR}(X) \approx \frac{1}{\langle X(t) \rangle} \left\langle \frac{dX(t)}{dt} \right\rangle \quad (\text{E2})$$

Values of $\text{RGR}(X)$ calculated in this way do not automatically satisfy the identities for relative growth rates of products, powers and quotients (Table 2).

In practice, the difference between $\text{RGR}(X)$ evaluated from Eqs. (E1) and (E2) is small, much less than the statistical uncertainty in $\text{RGR}(X)$ from either method. Equation (E2) is used for most RGR estimates in this paper. The exception is the attribution of contributions to $\text{RGR}(k_S)$ in Fig. 3, where Eq. (E1) is used for the observation estimates (black bars) and all model estimates, to ensure that model estimates satisfy constraints in Table 2.

The declining uptake rate of atmospheric CO₂ by land and ocean sinks

M. R. Raupach et al.

Title Page

Abstract

Introduction

Conclusions

References

Tables

Figures

⏪

⏩

◀

▶

Back

Close

Full Screen / Esc

Printer-friendly Version

Interactive Discussion



Implications of uncertainties in emissions

The uncertainty estimates for $RGR(AF)$ and $RGR(k_S)$ in Fig. 2 and Tables 3 and 4 reflect the stochastic variability associated with CO_2 growth rate, but not the uncertainty in data on CO_2 emissions from fossil fuels and other industrial processes (f_{FOSS}) and from net land use change (f_{LUC}). These are assessed as follows:

Uncertainty in CO_2 emissions from fossil fuels and other industrial processes (f_{FOSS}): the uncertainty in f_{FOSS} is estimated as $\pm 6\%$ (Andres et al., 2012; Marland, 2008). If this is random, the uncertainty propagated into $RGR(AF)$ and $RGR(k_S)$ is very small. However, some studies have suggested systematic biases for some countries, notably an underestimate of up to 20% in the late 1990s to early 2000s for China (Gregg et al., 2008). This would also be consistent with a suggested underestimate of global $f_{FOSS} + f_{LUC}$, for this period (Francey et al., 2010). Also, it has been suggested recently that there are significant uncertainties in Chinese emissions, particularly since 2005, from discrepancies between national and summed provincial accounts (Guan et al., 2012).

To assess the consequences of these possible revisions to f_{FOSS} , we computed $RGR(AF)$ and $RGR(k_S)$ using three alternative f_{FOSS} series (Fig. F1), in which f_{FOSS} was increased (1) between 1998 and 2003, (2) between 1993 and 2003, and (3) from 2000 onward using revised Chinese emissions based on provincial rather than national data (Guan et al., 2012). The resulting trends $RGR(AF)$ and $RGR(k_S)$ (Fig. F2), computed using data treatment (m, s, n) and the combined trend detection method, are slightly smaller in magnitude than the best estimates with primary f_{FOSS} data, but the differences are not statistically significant. Therefore, our conclusions are unaffected by any of the three possible revisions to f_{FOSS} (all of which are still speculative).

Uncertainty in CO_2 emissions from net land use change (f_{LUC}): it is well known that uncertainty in f_{LUC} is significant (Houghton, 2010, 2003) and propagates into the largest

The declining uptake rate of atmospheric CO_2 by land and ocean sinks

M. R. Raupach et al.

Title Page

Abstract

Introduction

Conclusions

References

Tables

Figures

⏪

⏩

◀

▶

Back

Close

Full Screen / Esc

Printer-friendly Version

Interactive Discussion

The declining uptake rate of atmospheric CO₂ by land and ocean sinks

M. R. Raupach et al.

[Title Page](#)

[Abstract](#)

[Introduction](#)

[Conclusions](#)

[References](#)

[Tables](#)

[Figures](#)

[⏪](#)

[⏩](#)

[◀](#)

[▶](#)

[Back](#)

[Close](#)

[Full Screen / Esc](#)

[Printer-friendly Version](#)

[Interactive Discussion](#)



uncertainty in AF trend estimates (Le Quéré et al., 2009; Raupach et al., 2008). The error on all f_{LUC} estimates is large, typically $\pm 50\%$. For estimation of both $\text{RGR}(\text{AF})$ and $\text{RGR}(k_{\text{S}})$, uncertainties arising from systematic biases in f_{LUC} data (both in level and trend) are more important than uncorrelated random errors in annual estimates. The primary data used here (Fig. B1) imply a downward revision of recent (since 2000) f_{LUC} from earlier estimates (Le Quéré et al., 2009). This is mainly attributable to methodological improvements in recently reported deforestation rates in the 2010 Food and Agriculture Organisation (FAO) Forest Resources Assessment (FAO, 2010), relative to the 2005 assessment (FAO, 2006) used earlier (Le Quéré et al., 2009). In Brazil, estimates for deforestation rates are now based on high-resolution remote sensing imagery, while latest estimates for Indonesia are based on data for 2003 and 2006, in contrast with 2005 estimates based on forecasts for this period. Recent studies in parts of the world that have dominated global deforestation inventories in past decades, including Brazil (Nepstad et al., 2009; Regalado, 2011) and Indonesia (Hansen et al., 2008), support the hypothesis that f_{LUC} has declined significantly through 2000–2009.

To assess the implications of uncertainty in f_{LUC} for trends AF and k_{S} , we replaced the primary f_{LUC} data (Friedlingstein et al., 2010) with 11 alternative annual time series from other assessments (Fig. F3 and Table F1). These alternative series are not independent, being based on just three sources of land cover data (FAO (FAO, 2010), SAGE (Ramankutty and Foley, 1999) and HYDE (Goldewijk, 2001)) and several carbon cycle models. Nevertheless, these series represent presently available estimates of global f_{LUC} from numerous investigators. All alternative f_{LUC} series end between 1990 and 2000, so each series was extrapolated in time by assuming either a linear decrease in f_{LUC} from 2000 onward at 0.03 PgC y^{-1} per year (consistent with our primary f_{LUC} data), or a constant f_{LUC} from the end of each alternative f_{LUC} series. These extrapolations, plotted in Fig. F3, are respectively denoted “Recent Fall” and “Recent Const”. Because of the likely decline in f_{LUC} since 2000, “Recent Fall” is the more likely scenario.

The resulting trends $RGR(AF)$ (Fig. F4) and $RGR(k_S)$ (Fig. F5), computed using data treatment (m, s, n) and the combined trend detection method, are slightly smaller in magnitude than the best estimates with primary f_{LUC} data, but the differences are not statistically significant. This indicates that uncertainty in f_{LUC} does not significantly affect our results.

Appendix G

Comparison with C4MIP results

Figure G1 compares the mean AF and its relative growth rate $RGR(AF)$ over 1959.0–2013.0 between data, SCCM and the 11 models in the C4MIP intercomparison (Friedlingstein et al., 2006), in both uncoupled and coupled modes. Figure G2 presents a similar comparison for mean sink rate k_S and the growth rate $RGR(k_S)$. For the magnitudes and growth rates of both AF and k_S , the agreement between data and SCCM results is good. In contrast, the agreement between data and all C4MIP models is poor. For the growth rate of AF, most (7 out of 11) C4MIP models in coupled mode predict the wrong sign (negative rather than positive as observed). For k_S , the negative growth rate is underestimated by all C4MIP models in coupled mode.

Comparisons of C4MIP projections with observations for AF and its growth rate have been presented previously (Le Quéré et al., 2009). Comparisons for the sink rate k_S and its growth rate are presented here for the first time.

Note on consistency: for the C4MIP results (available at annual time steps) it is necessary to estimate trends using Eq. (E2) in Appendix E, because many of the series change sign. Therefore, to maximise uniformity of the comparison, means and trends are estimated for the data and SCCM model results in Figs. G1 and G2 are also estimated using annual averages and Eq. (E2). This leads to small differences (much less than uncertainties in relative growth rates from data) between values of $RGR(AF)$ and $RGR(k_S)$ in Figs. G1 and G2 and Fig. 3, where estimates are based on annual data and

BGD

10, 18407–18454, 2013

The declining uptake rate of atmospheric CO₂ by land and ocean sinks

M. R. Raupach et al.

Title Page

Abstract

Introduction

Conclusions

References

Tables

Figures

⏪

⏩

◀

▶

Back

Close

Full Screen / Esc

Printer-friendly Version

Interactive Discussion



Eq. (E1). Reasons for using Eqs. (E1) and (E2) to estimate RGR in different contexts are given in Appendix E.

Acknowledgements. CO₂ data are provided by the Earth System Research Laboratory, US National Oceanic and Atmospheric Administration, and the CO₂ Program at the Scripps Institution of Oceanography. Data on fossil-fuel CO₂ emissions are provided by the Carbon Dioxide Information and Analysis Center (CDIAC), US Department of Energy. We thank W. Knorr for valuable comments. We acknowledge support to M. R. R. and J. G. C. from the Australian Climate Change Science Program of the Australian Government, to J. L. S. from the Carbon Mitigation Initiative of Princeton University, and to C. L. Q. from the European Union Framework Program 7 project CarboChange (264879). This work is a contribution to the Global Carbon Project.

References

- Ammann, C. M., Meehl, G. A., Washington, W. M., and Zender, C. S.: A monthly and latitudinally varying volcanic forcing dataset in simulations of 20th century climate, *Geophys. Res. Lett.*, 30, 1657, doi:10.1029/2003GL016875, 2003.
- Andres, R. J., Boden, T. A., Bréon, F.-M., Ciais, P., Davis, S., Erickson, D., Gregg, J. S., Jacobson, A., Marland, G., Miller, J., Oda, T., Olivier, J. G. J., Raupach, M. R., Rayner, P., and Treanton, K.: A synthesis of carbon dioxide emissions from fossil-fuel combustion, *Biogeosciences*, 9, 1845–1871, doi:10.5194/bg-9-1845-2012, 2012.
- Archer, D., Eby, M., Brovkin, V., Ridgwell, A., Cao, L., Mikolajewicz, U., Caldeira, K., Matsumoto, K., Munhoven, G., Montenegro, A., and Tokos, K.: Atmospheric lifetime of fossil fuel carbon dioxide, *Annu. Rev. Earth Pl. Sc.*, 37, 117–134, 2009.
- Bacastow, R. B. and Keeling, C. D.: Models to predict future atmospheric CO₂ concentrations, in: *Workshop on the Global Effects of Carbon Dioxide from Fossil Fuels*, edited by: Elliott, W. P. and Machta, L., United States Department of Energy, Washington DC, 1979.
- Ballantyne, A. P., Alden, C. B., Miller, J. B., Tans, P. P., and White, J. W. C.: Increase in observed net carbon dioxide uptake by land and oceans during the past 50 years, *Nature*, 488, 70–73, 2012.
- Boden, T. A., Marland, G., and Andres, R. J.: Global, regional and national fossil-fuel CO₂ emissions, Carbon Dioxide Information Analysis Center, Oak Ridge National Laboratory, US

The declining uptake rate of atmospheric CO₂ by land and ocean sinks

M. R. Raupach et al.

Title Page

Abstract

Introduction

Conclusions

References

Tables

Figures



Back

Close

Full Screen / Esc

Printer-friendly Version

Interactive Discussion



The declining uptake rate of atmospheric CO₂ by land and ocean sinks

M. R. Raupach et al.

Title Page

Abstract

Introduction

Conclusions

References

Tables

Figures

⏪

⏩

◀

▶

Back

Close

Full Screen / Esc

Printer-friendly Version

Interactive Discussion

Department of Energy, Oak Ridge, TN, USA, doi:10.3334/CDIAC/00001_V2013, http://cdiac.ornl.gov/trends/emis/meth_reg.html (last access: 23 November 2013), 2013.

Box, G., Jenkins, G. M., and Reinsel, G.: Time Series Analysis: Forecasting and Control, 3rd edn., Prentice Hall, Englewood Cliffs, NJ, 1994.

5 Canadell, J. G., Le Quééré, C., Raupach, M. R., Field, C. B., Buitenhuis, E. T., Ciais, P., Conway, T. J., Gillett, N. P., Houghton, R. A., and Marland, G.: Contributions to accelerating atmospheric CO₂ growth from economic activity, carbon intensity, and efficiency of natural sinks, *P. Natl. Acad. Sci. USA*, 104, 18866–18870, 2007.

10 Ciais, P., Gasser, T., Paris, J. D., Caldeira, K., Raupach, M. R., Canadell, J. G., Patwardhan, A., Friedlingstein, P., Piao, S., and Gitz, V.: Attributing the increase of atmospheric CO₂ to emitters and absorbers, *Nat. Clim. Change*, 3, 926–930, 2013.

FAO: Global Forest Resources Assessment 2005, Food and Agriculture Organization of the United Nations, Rome, 2006.

15 FAO: Global Forest Resources Assessment 2010, Food and Agriculture Organization of the United Nations, Rome, 2010.

Francey, R. J., Trudinger, C. M., van der Schoot, M., Krummel, P. B., Steele, L. P., and Langenfelds, R. L.: Differences between trends in atmospheric CO₂ and the reported trends in anthropogenic CO₂ emissions, *Tellus B*, 62, 316–328, 2010.

20 Friedlingstein, P., Cox, P., Betts, R., Bopp, L., von Bloh, W., Brovkin, V., Cadule, P., Doney, S., Eby, M., Fung, I., Bala, G., John, J., Jones, C., Joos, F., Kato, T., Kawamiya, M., Knorr, W., Lindsay, K., Matthews, H. D., Raddatz, T., Rayner, P., Reick, C., Roeckner, E., Schnitzler, K. G., Schnur, R., Strassmann, K., Weaver, A. J., Yoshikawa, C., and Zeng, N.: Climate–carbon cycle feedback analysis: results from the C4MIP model intercomparison, *J. Climate*, 19, 3337–3353, 2006.

25 Friedlingstein, P., Houghton, R. A., Marland, G., Hackler, J. L., Boden, T. A., Conway, T. J., Canadell, J. G., Raupach, M. R., Ciais, P., and Le Quééré, C.: Update on CO₂ emissions, *Nat. Geosci.*, 3, 811–812, 2010.

Frolicher, T. L., Joos, F., Raible, C. C., and Sarmiento, J. L.: Atmospheric CO₂ response to volcanic eruptions: the role of ENSO, season, and variability, *Global Biogeochem. Cy.*, 27, 239–251, 2013.

30 Gloor, M., Sarmiento, J. L., and Gruber, N.: What can be learned about carbon cycle climate feedbacks from the CO₂ airborne fraction?, *Atmos. Chem. Phys.*, 10, 7739–7751, doi:10.5194/acp-10-7739-2010, 2010.

The declining uptake rate of atmospheric CO₂ by land and ocean sinks

M. R. Raupach et al.

[Title Page](#)

[Abstract](#)

[Introduction](#)

[Conclusions](#)

[References](#)

[Tables](#)

[Figures](#)

[⏪](#)

[⏩](#)

[◀](#)

[▶](#)

[Back](#)

[Close](#)

[Full Screen / Esc](#)

[Printer-friendly Version](#)

[Interactive Discussion](#)

- Goldewijk, K. K.: Estimating global land use change over the past 300 years: the HYDE database 1, *Global Biogeochem. Cy.*, 15, 417–433, 2001.
- Gregg, J. S., Andres, R. J., and Marland, G.: China: emissions pattern of the world leader in CO₂ emissions from fossil fuel consumption and cement production, *Geophys. Res. Lett.*, 35, L08806, doi:10.1029/2007GL032887, 2008.
- Guan, D., Lui, Z., Geng, Y., Lindner, S., and Hubacek, K.: The gigatonne gap in China's carbon dioxide inventories, *Nat. Clim. Change*, 2, 672–675, doi:10.1038/NCLIMATE1560, 2012.
- Hansen, M. C., Stehman, S. V., Potapov, P. V., Loveland, T. R., Townshend, J. R. G., DeFries, R. S., Pittman, K. W., Arunarwati, B., Stolle, F., Steining, M. K., Carroll, M., and DiMiceli, C.: Humid tropical forest clearing from 2000 to 2005 quantified by using multitemporal and multiresolution remotely sensed data, *P. Natl. Acad. Sci. USA*, 105, 9439–9444, 2008.
- Harman, I. N., Trudinger, C. M., and Raupach, M. R.: SCCM – the Simple Carbon–Climate Model: Technical documentation, Centre for Australian Weather and Climate Research, Bureau of Meteorology and CSIRO, Melbourne, Australia, 2011.
- Hofmann, D. J., Butler, J. H., and Tans, P. P.: A new look at atmospheric carbon dioxide, *Atmos. Environ.*, 43, 2084–2086, 2009.
- Houghton, R. A.: Why are estimates of the terrestrial carbon balance so different?, *Glob. Change Biol.*, 9, 500–509, 2003.
- Houghton, R. A.: How well do we know the flux of CO₂ from land-use change?, *Tellus B*, 62, 337–351, 2010.
- IPCC: *Climate Change 2007: Synthesis Report*, Cambridge University Press, Cambridge, UK and New York, NY, USA, 2007.
- Jones, C. D. and Cox, P. M.: Modeling the volcanic signal in the atmospheric CO₂ record, *Global Biogeochem. Cy.*, 15, 453–465, 2001.
- Joos, F., Bruno, M., Fink, R., Siegenthaler, U., Stocker, T. F., and Le Quéré, C.: An efficient and accurate representation of complex oceanic and biospheric models of anthropogenic carbon uptake, *Tellus B*, 48, 397–417, 1996.
- Joos, F., Roth, R., Fuglestad, J. S., Peters, G. P., Enting, I. G., von Bloh, W., Brovkin, V., Burke, E. J., Eby, M., Edwards, N. R., Friedrich, T., Frölicher, T. L., Halloran, P. R., Holden, P. B., Jones, C., Kleinen, T., Mackenzie, F. T., Matsumoto, K., Meinshausen, M., Plattner, G.-K., Reisinger, A., Segschneider, J., Shaffer, G., Steinacher, M., Strassmann, K., Tanaka, K., Timmermann, A., and Weaver, A. J.: Carbon dioxide and climate impulse re-

The declining uptake rate of atmospheric CO₂ by land and ocean sinks

M. R. Raupach et al.

Title Page

Abstract

Introduction

Conclusions

References

Tables

Figures

⏪

⏩

◀

▶

Back

Close

Full Screen / Esc

Printer-friendly Version

Interactive Discussion

- response functions for the computation of greenhouse gas metrics: a multi-model analysis, *Atmos. Chem. Phys.*, 13, 2793–2825, doi:10.5194/acp-13-2793-2013, 2013.
- Keeling, C. D. and Revelle, R.: Effects of El-Nino Southern Oscillation on the atmospheric content of carbon-dioxide, *Meteoritics*, 20, 437–450, 1985.
- 5 Keeling, C. D., Piper, S. C., Bacastow, R. B., Wahlen, M., Whorf, T. P., Heimann, M., and Meijer, H. A.: Exchanges of Atmospheric CO₂ and ¹³CO₂ with the Terrestrial Biosphere and Oceans From 1978 to 2000. I. Global Aspects, *Scripps Institution of Oceanography, San Diego*, 88 pp., 2001.
- Keeling, C. D., Piper, S. C., Bacastow, R. B., Wahlen, M., Whorf, T. P., Heimann, M., and Meijer, H. A.: Atmospheric CO₂ and ¹³CO₂ exchange with the terrestrial biosphere and oceans from 1978 to 2000: observations and carbon cycle implications, in: *A History of Atmospheric CO₂ and Its Effects on Plants, Animals, and Ecosystems*, edited by: Ehleringer, J. R., Cerling, T. E., and Dearing, M. D., Springer Verlag, New York, 2005.
- 10 Knorr, W.: Is the airborne fraction of anthropogenic CO₂ emissions increasing?, *Geophys. Res. Lett.*, 36, L21710, doi:10.1029/2009GL040613, 2009.
- Le Quéré, C., Rodenbeck, C., Buitenhuis, E. T., Conway, T. J., Langenfelds, R., Gomez, A., Labuschagne, C., Ramonet, M., Nakazawa, T., Metzl, N., Gillett, N., and Heimann, M.: Saturation of the Southern Ocean CO₂ sink due to recent climate change, *Science*, 316, 1735–1738, 2007.
- 20 Le Quéré, C., Raupach, M. R., Canadell, J. G., Marland, G., Bopp, L., Ciais, P., Conway, T. J., Doney, S. C., Feely, R. A., Foster, P., Friedlingstein, P., Gurney, K. R., Houghton, R. A., House, J. I., Huntingford, C., Levy, P. E., Lomas, M. R., Majkut, J., Metzl, N., Ometto, J., Peters, G. P., Prentice, I. C., Randerson, J. T., Running, S. W., Sarmiento, J. L., Schuster, U., Sitch, S., Takahashi, T., Viovy, N., van der Werf, G. R., and Woodward, F. I.: Trends in the sources and sinks of carbon dioxide, *Nat. Geosci.*, 2, 831–836, 2009.
- 25 Le Quéré, C., Andres, R. J., Boden, T., Conway, T., Houghton, R. A., House, J. I., Marland, G., Peters, G. P., van der Werf, G. R., Ahlström, A., Andrew, R. M., Bopp, L., Canadell, J. G., Ciais, P., Doney, S. C., Enright, C., Friedlingstein, P., Huntingford, C., Jain, A. K., Jourdain, C., Kato, E., Keeling, R. F., Klein Goldewijk, K., Levis, S., Levy, P., Lomas, M., Poulter, B., Raupach, M. R., Schwinger, J., Sitch, S., Stocker, B. D., Viovy, N., Zaehle, S., and Zeng, N.: The global carbon budget 1959–2011, *Earth Syst. Sci. Data*, 5, 165–185, doi:10.5194/essd-5-165-2013, 2013.
- 30

The declining uptake rate of atmospheric CO₂ by land and ocean sinks

M. R. Raupach et al.

Title Page

Abstract

Introduction

Conclusions

References

Tables

Figures

⏪

⏩

◀

▶

Back

Close

Full Screen / Esc

Printer-friendly Version

Interactive Discussion

- Lewis, E. and Wallace, D. J.: Program Developed for CO₂ System Calculations, Carbon Dioxide Information Analysis Center, Oak Ridge National Laboratory, Oak Ridge, Tennessee, 38 pp., 1998.
- Li, S. and Jarvis, A.: Long run surface temperature dynamics of an A-OGCM: the HadCM3 4xCO₂ forcing experiment revisited, *Clim. Dynam.*, 33, 817–825, 2009.
- Marland, G.: Uncertainties in accounting for CO₂ from fossil fuels, *J. Ind. Ecol.*, 12, 136–139, 2008.
- McGuire, A. D., Sitch, S., Clein, J. S., Dargaville, R., Esser, G., Foley, J. A., Heimann, M., Joos, F., Kaplan, J., Kicklighter, D. W., Meier, R. A., Melillo, J. M., Moore, B., Prentice, I. C., Ramankutty, N., Reichenau, T., Schloss, A., Tian, H., Williams, L. J., and Wittenberg, U.: Carbon balance of the terrestrial biosphere in the twentieth century: analyses of CO₂, climate and land use effects with four process-based ecosystem models 1, *Global Biogeochem. Cy.*, 15, 183–206, 2001.
- Nepstad, D., Soares, B. S., Merry, F., Lima, A., Moutinho, P., Carter, J., Bowman, M., Cattaneo, A., Rodrigues, H., Schwartzman, S., McGrath, D. G., Stickler, C. M., Lubowski, R., Pires-Cabezas, P., Rivero, S., Alencar, A., Almeida, O., and Stella, O.: The end of deforestation in the Brazilian Amazon, *Science*, 326, 1350–1351, 2009.
- NOAA-ESRL: Trends in Atmospheric Carbon Dioxide, Global Monitoring Division, Earth System Research Laboratory, National Oceanic and Atmospheric Administration, Boulder, CO, USA, <http://www.esrl.noaa.gov/gmd/ccgg/trends/> (last access: 23 November 2013), 2013.
- Oeschger, H., Siegenthaler, U., and Heimann, M.: The carbon cycle and its perturbations by man, in: *Interactions of Energy and Climate*, edited by: Bach, W., Pankrath, J., and Williams, J., Reidel, Dordrecht, 1980.
- Piao, S. L., Ciais, P., Friedlingstein, P., de Noblet-Ducoudre, N., Cadule, P., Viovy, N., and Wang, T.: Spatiotemporal patterns of terrestrial carbon cycle during the 20th century, *Global Biogeochem. Cy.*, 23, GB4026, doi:10.1029/2008GB003339, 2009.
- Ramankutty, N. and Foley, J. A.: Estimating historical changes in global land cover: croplands from 1700 to 1992, *Global Biogeochem. Cy.*, 13, 997–1027, 1999.
- Raupach, M. R.: The exponential eigenmodes of the carbon–climate system, and their implications for ratios of responses to forcings, *Earth Syst. Dynam.*, 4, 31–49, doi:10.5194/esd-4-31-2013, 2013.

The declining uptake rate of atmospheric CO₂ by land and ocean sinks

M. R. Raupach et al.

[Title Page](#)

[Abstract](#)

[Introduction](#)

[Conclusions](#)

[References](#)

[Tables](#)

[Figures](#)

[⏪](#)

[⏩](#)

[◀](#)

[▶](#)

[Back](#)

[Close](#)

[Full Screen / Esc](#)

[Printer-friendly Version](#)

[Interactive Discussion](#)

Raupach, M. R., Canadell, J. G., and Le Quéré, C.: Anthropogenic and biophysical contributions to increasing atmospheric CO₂ growth rate and airborne fraction, *Biogeosciences*, 5, 1601–1613, doi:10.5194/bg-5-1601-2008, 2008.

Raupach, M. R., Canadell, J. G., Ciais, P., Friedlingstein, P., Rayner, P. J., and Trudinger, C. M.: The relationship between peak warming and cumulative CO₂ emissions, and its use to quantify vulnerabilities in the carbon–climate–human system, *Tellus B*, 63, 145–164, 2011.

Regalado, A.: Brazil says rate of deforestation in the Amazon continues to plunge, *Science*, 329, 1270–1271, 2011.

Sarmiento, J. L., Gloor, M., Gruber, N., Beaulieu, C., Jacobson, A. R., Mikaloff Fletcher, S. E., Pacala, S., and Rodgers, K.: Trends and regional distributions of land and ocean carbon sinks, *Biogeosciences*, 7, 2351–2367, doi:10.5194/bg-7-2351-2010, 2010.

Scripps CO₂ Program: Atmospheric CO₂ data, Scripps Institution of Oceanography, San Diego, CA, USA, <http://scrippsco2.ucsd.edu/data/data.html>, (last access: 23 November 2013), 2013.

Shevliakova, E., Pacala, S. W., Malyshev, S., Hurtt, G. C., Milly, P. C. D., Caspersen, J. P., Sentman, L. T., Fisk, J. P., Wirth, C., and Crevoisier, C.: Carbon cycling under 300 years of land use change: importance of the secondary vegetation sink 1, *Global Biogeochem. Cy.*, 23, GB2022, doi:10.1029/2007GB003176, 2009.

Strassmann, K. M., Joos, F., and Fischer, G.: Simulating effects of land use changes on carbon fluxes: past contributions to atmospheric CO₂ increases and future commitments due to losses of terrestrial sink capacity 1, *Tellus B*, 60, 583–603, 2008.

Tans, P.: An accounting of the observed increase in oceanic and atmospheric CO₂ and an outlook for the future, *Oceanography*, 22, 26–35, 2009.

UNFCCC: Methodological Issues: Scientific and Methodological Assessment of Contributions to Climate Change, Subsidiary Body for Scientific and Technological Advice, United Nations Framework Convention on Climate Change, New Delhi, 27 pp., 2002.

Van Minnen, J. G., Goldewijk, K. K., Stehfest, E., Eickhout, B., Van Drecht, G., and Leemans, R.: The importance of three centuries of land-use change for the global and regional terrestrial carbon cycle, *Climatic Change*, 97, 123–144, 2009.

The declining uptake rate of atmospheric CO₂ by land and ocean sinks

M. R. Raupach et al.

Table 1. Definitions of quantities. Notation: c_A , the excess CO₂ in mass units, is the perturbation atmospheric CO₂ store in PgC (equal to $2.127([\text{CO}_2] - [\text{CO}_2]_q)$, where $[\text{CO}_2]$ is the CO₂ mixing ratio (ppm), and $[\text{CO}_2]_q = 278 \text{ ppm} = [\text{CO}_2]$ at preindustrial equilibrium); $c'_A = dc_A/dt$ is the atmospheric CO₂ accumulation rate in PgCyr⁻¹; f_E is the total CO₂ emission flux in PgCyr⁻¹ (the sum of emissions from fossil fuels and other industry, f_{Fossil} , and from net land use change, f_{LUC}); f_L and f_M are the CO₂ land–air (L) and ocean–air (M, marine) exchange fluxes in PgCyr⁻¹; f_{IS} is the total (land plus ocean) CO₂ sink flux. All fluxes are positive upward (surface to atmosphere) except f_{IS} , which is positive downward to denote a CO₂ sink. The AF is often alternatively defined as an “apparent airborne fraction” c'_A/f_{Fossil} (Oeschger et al., 1980); use of this alternative definition would change numerical trend estimates for AF but not our fundamental conclusions about attribution. The definition used here allows the anthropogenic contribution to CO₂ growth from land use change to be distinguished from the terrestrial carbon sink (Le Quéré et al., 2009; Raupach et al., 2008).

Physical concept	Defining equation	Eq.
Atmospheric CO ₂ mass balance (all terms in PgC yr ⁻¹)	$c'_A = f_E + f_L + f_M = f_E - f_{\text{IS}}$ (with $c'_A = dc_A/dt$, $f_E = f_{\text{Fossil}} + f_{\text{LUC}}$, $f_{\text{IS}} = -f_L - f_M$)	(2)
Airborne and sink fractions (dimensionless)	$\text{AF} = c'_A/f_E$ $\text{SF} = f_{\text{IS}}/f_E = 1 - \text{AF}$	(3)
CO ₂ sink rate (yr ⁻¹)	$k_S = f_{\text{IS}}/c_A = (-f_L - f_M)/c_A = (f_E - c'_A)/c_A$	(4)
Relationship between AF and k_S	$k_S = \text{SF} f_E/c_A = (1 - \text{AF})f_E/c_A$	(5)

Title Page

Abstract

Introduction

Conclusions

References

Tables

Figures

◀

▶

◀

▶

Back

Close

Full Screen / Esc

Printer-friendly Version

Interactive Discussion

The declining uptake rate of atmospheric CO₂ by land and ocean sinks

M. R. Raupach et al.

Table 2. Relationships among the relative growth rates of AF and k_S . Equation (6) gives general mathematical identities for relative growth rates of products and quotients. Equations (7) and (8) apply these identities to Eqs. (3) and (4), respectively, to establish relationships between RGR(AF) and RGR(k_S).

Concept	Defining equation	Eq.
General rules for relative growth rates of powers, products and quotients	$\text{RGR}(xy/z) = \text{RGR}(x) + \text{RGR}(y) - \text{RGR}(z)$ with $\text{RGR}(x(t)) = \frac{d(\ln x(t))}{dt} = \frac{x'(t)}{x(t)}$	(6)
Relationships between relative growth rates of AF and k_S	$\text{RGR}(AF) = \text{RGR}(c'_A) - \text{RGR}(f_E)$	(7)
	$\text{RGR}(k_S) = \text{RGR}(f_{IS}) - \text{RGR}(c_A)$ $= \text{RGR}(SF) + \text{RGR}(f_E) - \text{RGR}(c_A)$	(8)

[Title Page](#)
[Abstract](#)
[Introduction](#)
[Conclusions](#)
[References](#)
[Tables](#)
[Figures](#)
[Back](#)
[Close](#)
[Full Screen / Esc](#)
[Printer-friendly Version](#)
[Interactive Discussion](#)

The declining uptake rate of atmospheric CO₂ by land and ocean sinks

M. R. Raupach et al.

[Title Page](#)

[Abstract](#)

[Introduction](#)

[Conclusions](#)

[References](#)

[Tables](#)

[Figures](#)

[⏪](#)

[⏩](#)

[◀](#)

[▶](#)

[Back](#)

[Close](#)

[Full Screen / Esc](#)

[Printer-friendly Version](#)

[Interactive Discussion](#)



Table 3. Estimates of the relative growth rate of the airborne fraction over March 1958 to December 2012, evaluated using Eq. (E2). Rows distinguish different data treatments, columns distinguish different trend estimation methods. Ranges are $\pm 1\sigma$ confidence intervals; P values in brackets give probability of positive trend. The best estimate (from data treatment AF(m, s, n)) with the combined trend estimation method) is shown in bold.

	RGR(AF) (%yr ⁻¹)			
	Regression	Stochastic	Bootstrap	Combined
AF(a)	0.27 ± 0.29 ($P = 0.64$)			
AF(m)	0.27 ± 0.27 ($P = 0.68$)	0.28 ± 0.30 ($P = 0.83$)	0.35 ^a	0.33 ± 0.30 ($P = 0.87$)
AF(m, n)	0.27 ± 0.26 ($P = 0.70$)	0.27 ± 0.21 ($P = 0.90$)	0.24 ^a	0.23 ± 0.20 ($P = 0.89$)
AF(m, s)	0.29 ^b	0.27 ± 0.35 ($P = 0.78$)	0.35 ^a	0.35 ± 0.36 ($P = 0.85$)
AF(m, s, n)	0.29 ^b	0.29 ± 0.20 ($P = 0.92$)	0.27 ^a	0.27 ± 0.20 ($P = 0.91$)

^a The bootstrap trend estimation method does not return confidence intervals or P values.

^b For data treatments involving smoothing of monthly data, AF(m, s) and AF(m, s, n), regression yields spuriously small confidence intervals (not shown) because of temporal autocorrelation of time series.

The declining uptake rate of atmospheric CO₂ by land and ocean sinks

M. R. Raupach et al.

[Title Page](#)

[Abstract](#)

[Introduction](#)

[Conclusions](#)

[References](#)

[Tables](#)

[Figures](#)

⏪

⏩

◀

▶

[Back](#)

[Close](#)

[Full Screen / Esc](#)

[Printer-friendly Version](#)

[Interactive Discussion](#)



Table 4. Estimates of the relative growth rate of the CO₂ sink rate k_S over March 1958 to December 2012, evaluated using Eq (E2). Rows distinguish different data treatments, columns distinguish different trend estimation methods. Ranges are $\pm 1\sigma$ confidence intervals. All P values (probability of negative trend) exceed 0.998 and are not shown. The best estimate, with $P > 0.999$, is shown in bold.

	Regression	RGR(k_S) (%yr ⁻¹)		
		Stochastic	Bootstrap	Combined
$k_S(a)$	-0.78 ± 0.23			
$k_S(m)$	-0.77 ± 0.21	-0.78 ± 0.24	-0.97^a	-0.99 ± 0.24
$k_S(m, n)$	-0.77 ± 0.21	-0.77 ± 0.17	-0.90^a	-0.90 ± 0.16
$k_S(m, s)$	-0.81^b	-0.81 ± 0.29	-0.99^a	-0.99 ± 0.29
$k_S(m, s, n)$	-0.80^b	-0.81 ± 0.16	-0.94^a	-0.93 ± 0.17

^{a, b} See Table 3 caption.

The declining uptake rate of atmospheric CO₂ by land and ocean sinks

M. R. Raupach et al.

Table F1. Details of AF trend estimates from 11 alternative time series for CO₂ emissions from net land use change, f_{LUC} . Trends are evaluated using Eq. (E2). Data are extrapolated from the last point in each series assuming either “Recent Fall” (constant f_{LUC} to 2000 and linear decline from 2000 to 2012 at 0.03 PgCyr⁻¹ per year, with the constraint that f_{LUC} not fall below the lesser of the last point and 0.5 PgCyr⁻¹); or “Recent Const” (constant f_{LUC} to 2012). Time series are plotted in Fig. F3. The combined trend estimation method is used for all AF trend estimates. Ranges are $\pm 1\sigma$ confidence intervals; P values in brackets give probability of positive trend.

Ident	No	Lead author (references in caption)	Carbon cycle model	Land cover data	Last year	RGR(AF) (%yr ⁻¹) (Recent fall)	RGR(AF) (%yr ⁻¹) (Recent const)
Hou08	1	Houghton	Houghton	FAO	2008	0.16 ± 0.20 ($P = 0.81$)	0.16 ± 0.20 ($P = 0.81$)
vanMd	2	Van Minnen	IMAGE2	HYDE ^a	2000	0.17 ± 0.20 ($P = 0.82$)	0.15 ± 0.20 ($P = 0.78$)
vanMp	3	Van Minnen	IMAGE2	HYDE ^b	2000	0.20 ± 0.20 ($P = 0.86$)	0.18 ± 0.20 ($P = 0.82$)
IBIS	4	McGuire	IBIS	SAGE	1992	0.23 ± 0.21 ($P = 0.88$)	0.21 ± 0.22 ($P = 0.85$)
HRBM	5	McGuire	HRBM	SAGE	1992	0.26 ± 0.21 ($P = 0.90$)	0.24 ± 0.21 ($P = 0.88$)
LPJ	6	McGuire	LPJ	SAGE	1992	0.41 ± 0.21 ($P = 0.98$)	0.39 ± 0.22 ($P = 0.96$)
TEM	7	McGuire	TEM	SAGE	1992	0.24 ± 0.20 ($P = 0.89$)	0.24 ± 0.20 ($P = 0.89$)
Piao	8	Piao	ORCHIDEE	SAGE	1992	0.22 ± 0.22 ($P = 0.85$)	0.20 ± 0.23 ($P = 0.82$)
ShS1	9	Shevliakova	LM3V	SAGE/HYDE	1990	0.29 ± 0.20 ($P = 0.93$)	0.27 ± 0.21 ($P = 0.91$)
ShH1	10	Shevliakova	LM3V	HYDE	1990	0.20 ± 0.21 ($P = 0.84$)	0.17 ± 0.22 ($P = 0.80$)
Str08	11	Strassmann	BernCC	HYDE	2000	0.25 ± 0.20 ($P = 0.90$)	0.23 ± 0.20 ($P = 0.88$)

^a Default.

^b Pasture.

References: Houghton (2010), McGuire et al. (2001), Piao et al. (2009), Shevliakova et al. (2009), Strassmann et al. (2008) Van Minnen et al. (2009).

Title Page

Abstract

Introduction

Conclusions

References

Tables

Figures

⏪

⏩

◀

▶

Back

Close

Full Screen / Esc

Printer-friendly Version

Interactive Discussion

The declining uptake rate of atmospheric CO₂ by land and ocean sinks

M. R. Raupach et al.

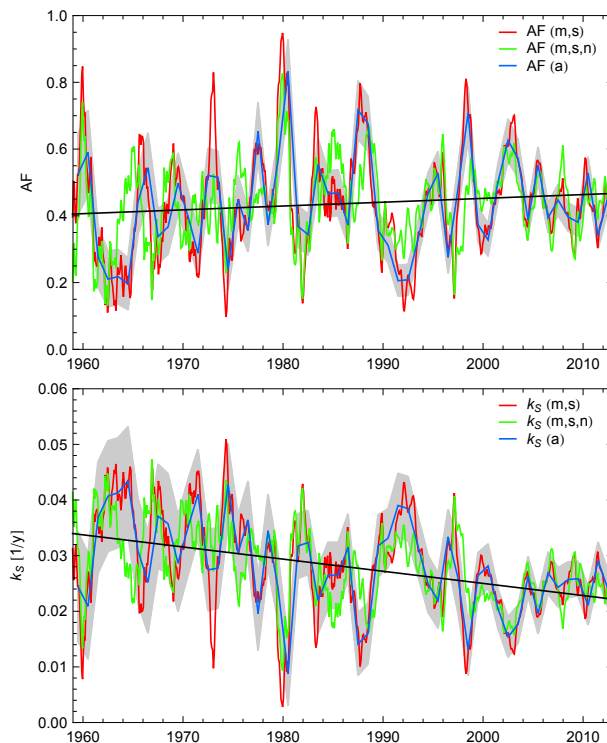


Fig. 1. Upper panel: (red) monthly airborne fraction $AF(m, s)$ with 15 month running mean smoothing; (green) $AF(m, s, n)$ with removal of noise correlated with El Niño-Southern Oscillation (ENSO); (blue) annual $AF(a)$; (black) best-estimate trend line from $AF(m, s, n)$ with the combined method. Lower panel: (red) monthly CO₂ sink rate $k_S(m, s)$ with 15 month running mean smoothing; (green) monthly $k_S(m, s, n)$ with ENSO-correlated noise removal; (blue) annual $k_S(a)$; (black) best-estimate trend line from $k_S(m, s, n)$ with the combined method. Grey bands indicate $\pm 1\sigma$ ranges due to observation uncertainties in emissions and CO₂ concentrations, referenced to annual (a) series.

[Title Page](#)
[Abstract](#)
[Introduction](#)
[Conclusions](#)
[References](#)
[Tables](#)
[Figures](#)
[Back](#)
[Close](#)
[Full Screen / Esc](#)
[Printer-friendly Version](#)
[Interactive Discussion](#)

The declining uptake rate of atmospheric CO₂ by land and ocean sinks

M. R. Raupach et al.

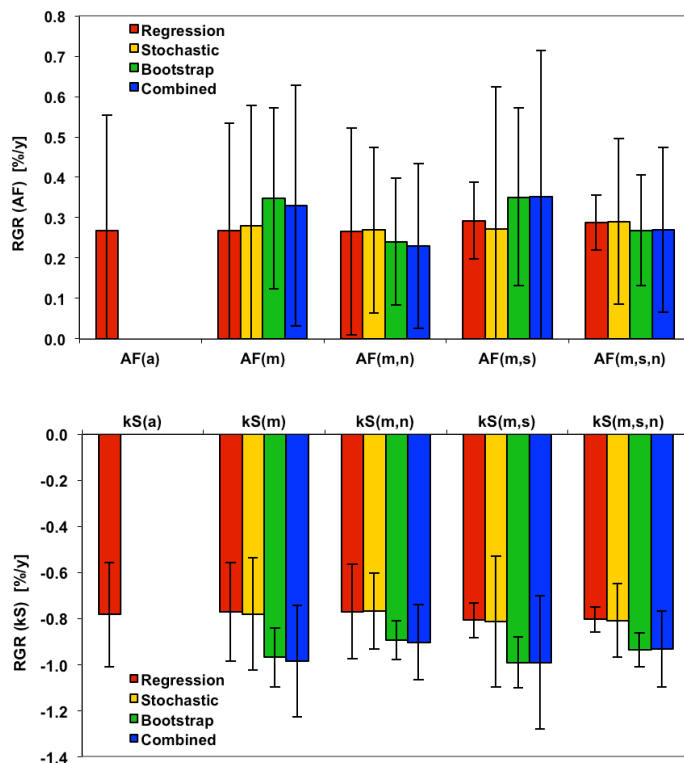


Fig. 2. Estimates of $RGR(AF)$ and $RGR(k_S)$ over 1959.0–2013.0, from five data treatments and four trend estimation methods. Error bars show $\pm 1\sigma$ confidence intervals. Trends are estimated using Eq. (E2). P values for trend significance are given in Tables 3 and 4. Data treatments are described in detail in Appendix C, and trend estimation methods in Appendix D. Best trend estimates in the text are from the combined method applied to data treatment (m, s, n) , the rightmost blue bar in each panel.

The declining uptake rate of atmospheric CO₂ by land and ocean sinks

M. R. Raupach et al.

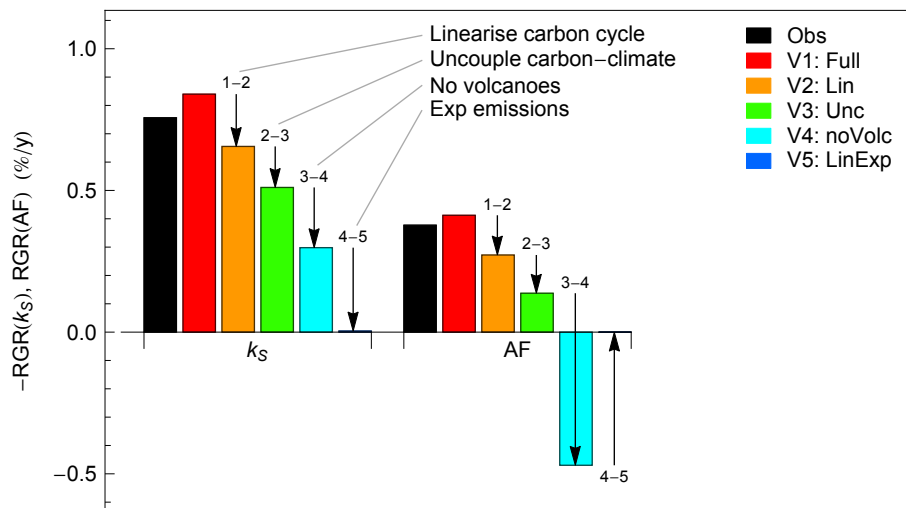


Fig. 3. Relative growth rates of k_S and AF over 1959.0–2013.0, at 5 accumulating levels of model simplification: (1) full model, (2) linearised, (3) uncoupled, (4) no volcanoes, (5) LinExp idealisation. The labelled vertical arrows indicate the model simplification occurring at each step (e.g. linearisation of the carbon cycle in the step from V1 to V2). Corresponding trajectories of CO₂ and temperature are shown in Fig. 6, and trajectories of k_S and AF in Fig. 7. Note that $RGR(k_S)$ is negative and is plotted with reversed sign. Trends are estimated using Eq. (E1) in Appendix E, to ensure consistency with identities for relative growth rates of products (Table 2).

Title Page

Abstract

Introduction

Conclusions

References

Tables

Figures

⏪

⏩

◀

▶

Back

Close

Full Screen / Esc

Printer-friendly Version

Interactive Discussion

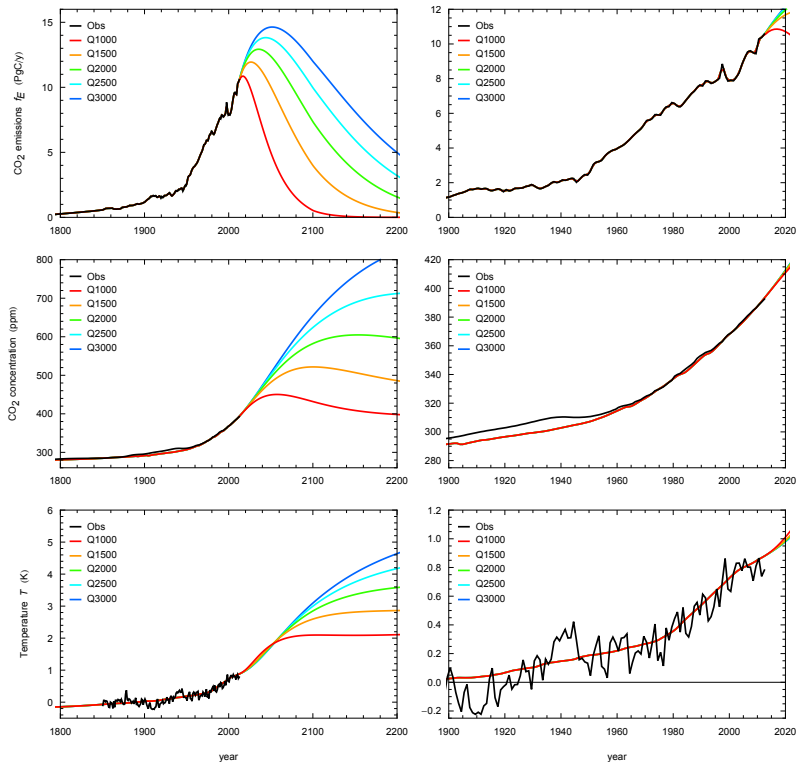


Fig. 4. Total CO₂ emissions (f_E , top row) and SCCM predictions for CO₂ concentration (middle row) and temperature (bottom row), with analytic scenarios for future emissions of CO₂ and non-CO₂ gases (CH₄, N₂O, CFCs) such that the all-time cumulative total CO₂ emission $Q_E(\infty)$ takes values from 1000 to 3000 PgC. Scenarios and model details (including treatment of aerosols) are given in Raupach (2013). Left panels show plots against time from 1800 to 2200, right panels zoom in to the period 1900–2020 to compare model with data. This figure is a variation with added detail of Fig. 6 in Raupach (2013).

The declining uptake rate of atmospheric CO₂ by land and ocean sinks

M. R. Raupach et al.

Title Page

Abstract Introduction

Conclusions References

Tables Figures

◀ ▶

◀ ▶

Back Close

Full Screen / Esc

Printer-friendly Version

Interactive Discussion



The declining uptake rate of atmospheric CO₂ by land and ocean sinks

M. R. Raupach et al.

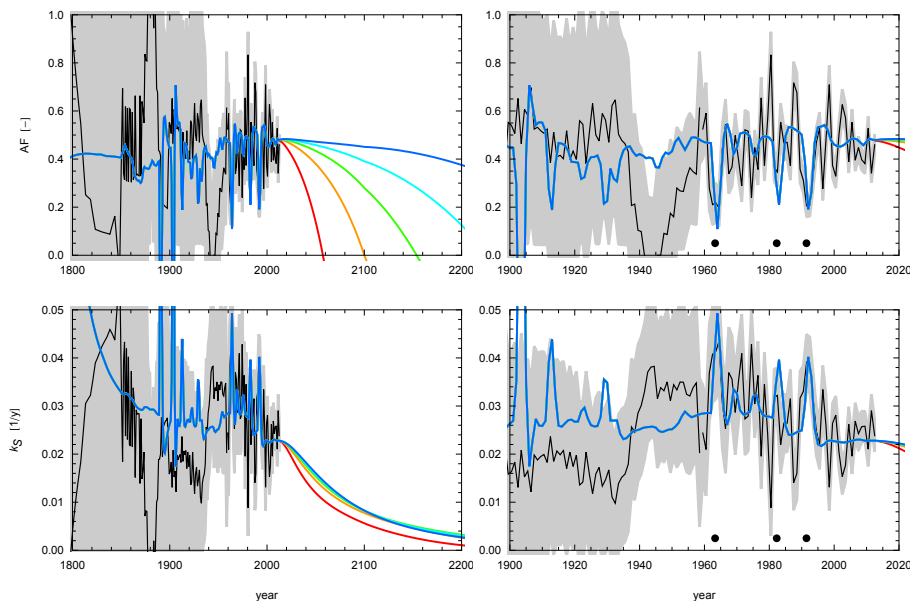


Fig. 5. Trajectories of AF and k_S (upper and lower rows), for the analytic scenarios shown in Fig. 4. Dots in right (zoom) panels indicate times of major volcanic eruptions since 1959 (Agung, El Chichon, Pinatubo). Black lines are observations; grey bands indicate $\pm 1\sigma$ ranges due to observation uncertainties in emissions and CO₂ concentrations. Historical SCCM results (prior to 2013.0) appear as blue in all panels. Other details follow Fig. 4. This figure is a variation with added detail of Fig. 7 in Raupach (2013).

The declining uptake rate of atmospheric CO₂ by land and ocean sinks

M. R. Raupach et al.

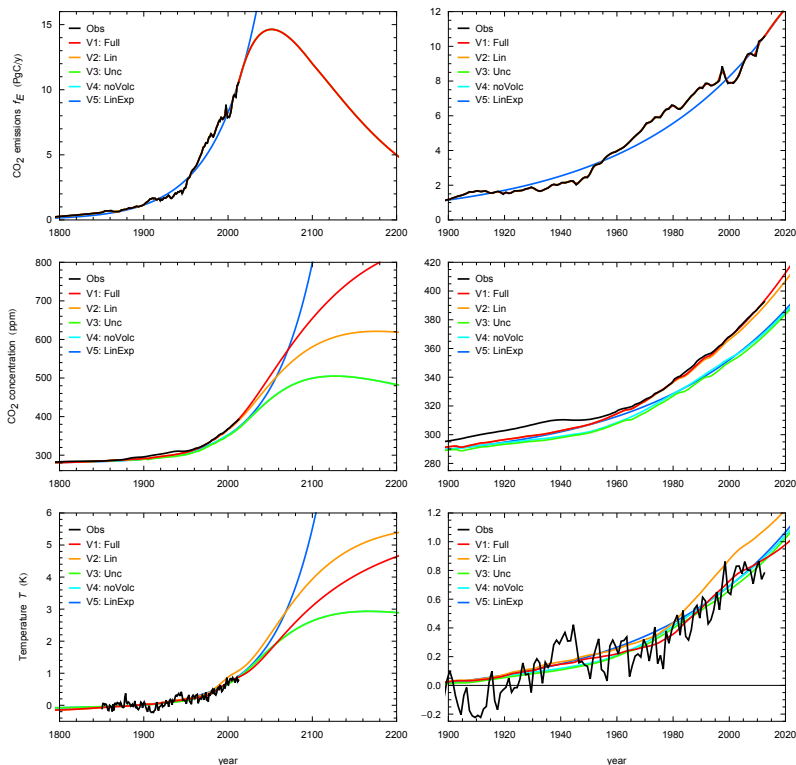


Fig. 6. Total CO₂ emissions (f_E , top row) and SCCM predictions for CO₂ concentration (middle row) and temperature (bottom row), at 5 accumulating levels of model simplification, as in Fig. 3: (1) full model, (2) linearised, (3) uncoupled, (4) no volcanoes, (5) LinExp idealisation. The emissions scenario is the case $Q_E(\infty) = 3000$ PgC in Fig. 4. Other details follow Fig. 4. This figure is a variation with added detail of Fig. 8 in Raupach (2013), using orderings for model simplification steps consistent with this paper.

[Title Page](#)
[Abstract](#)
[Introduction](#)
[Conclusions](#)
[References](#)
[Tables](#)
[Figures](#)
[Back](#)
[Close](#)
[Full Screen / Esc](#)
[Printer-friendly Version](#)
[Interactive Discussion](#)

The declining uptake rate of atmospheric CO₂ by land and ocean sinks

M. R. Raupach et al.

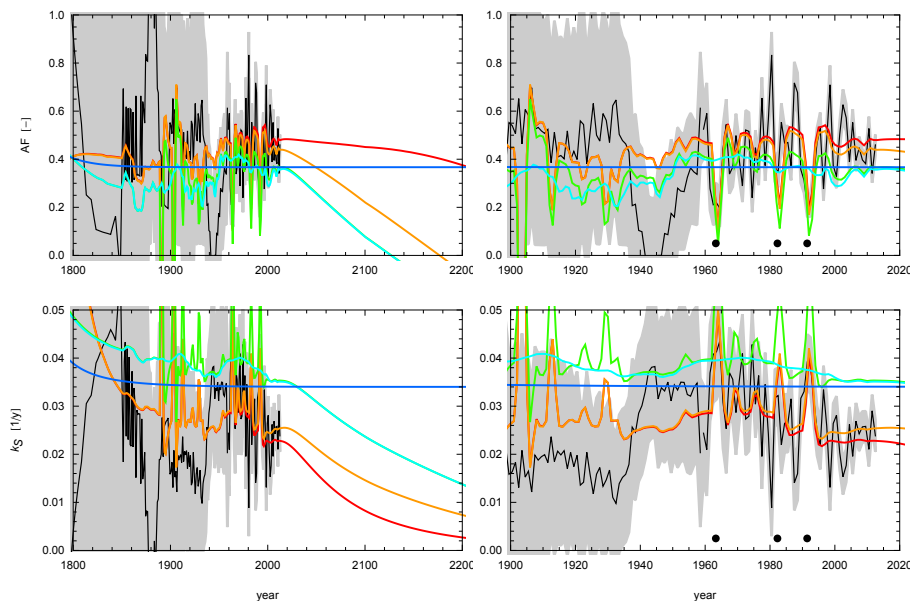


Fig. 7. Trajectories of AF and k_S (upper and lower rows), for the model simplification cases shown in Figs. 3 and 6. Dots in right (zoom) panels indicate times of major volcanic eruptions since 1959 (Agung, El Chichon, Pinatubo). Other details as in Figs. 4 and 5. This figure is a variation with added detail of Fig. 9 in Raupach (2013), using orderings for model simplification steps consistent with this paper.

[Title Page](#)
[Abstract](#)
[Introduction](#)
[Conclusions](#)
[References](#)
[Tables](#)
[Figures](#)
[⏪](#)
[⏩](#)
[◀](#)
[▶](#)
[Back](#)
[Close](#)
[Full Screen / Esc](#)
[Printer-friendly Version](#)
[Interactive Discussion](#)

The declining uptake rate of atmospheric CO₂ by land and ocean sinks

M. R. Raupach et al.

Title Page

Abstract

Introduction

Conclusions

References

Tables

Figures



Back

Close

Full Screen / Esc

Printer-friendly Version

Interactive Discussion

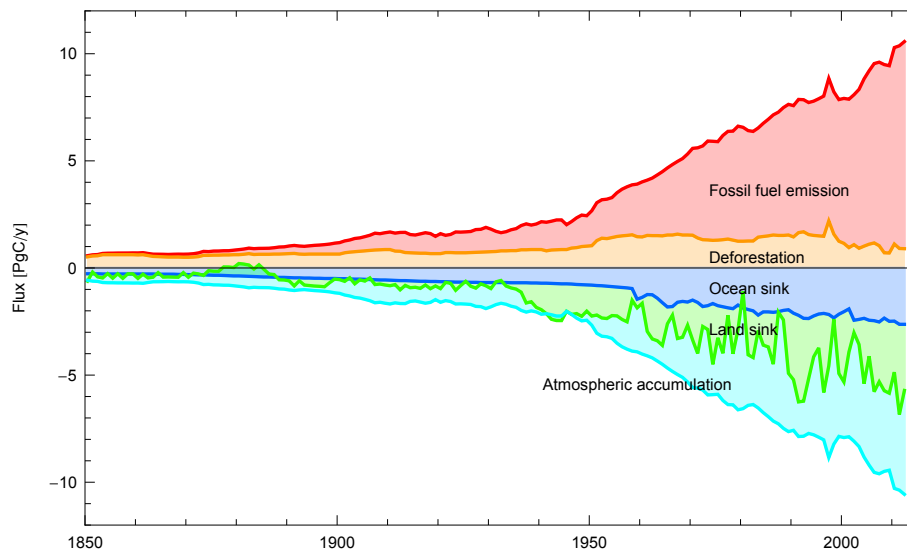


Fig. B1. Global atmospheric CO₂ budget for 1959.0–2013.0 (Table 1, Eq. 2), showing stacked time series of annual f_{FOSS} , annual f_{LUC} , annual CO₂ accumulation $c'_A = dc_A/dt$, annual land–air exchange flux f_L , and annual ocean–air exchange flux f_M .

The declining uptake rate of atmospheric CO₂ by land and ocean sinks

M. R. Raupach et al.

Title Page

Abstract

Introduction

Conclusions

References

Tables

Figures

⏪

⏩

◀

▶

Back

Close

Full Screen / Esc

Printer-friendly Version

Interactive Discussion

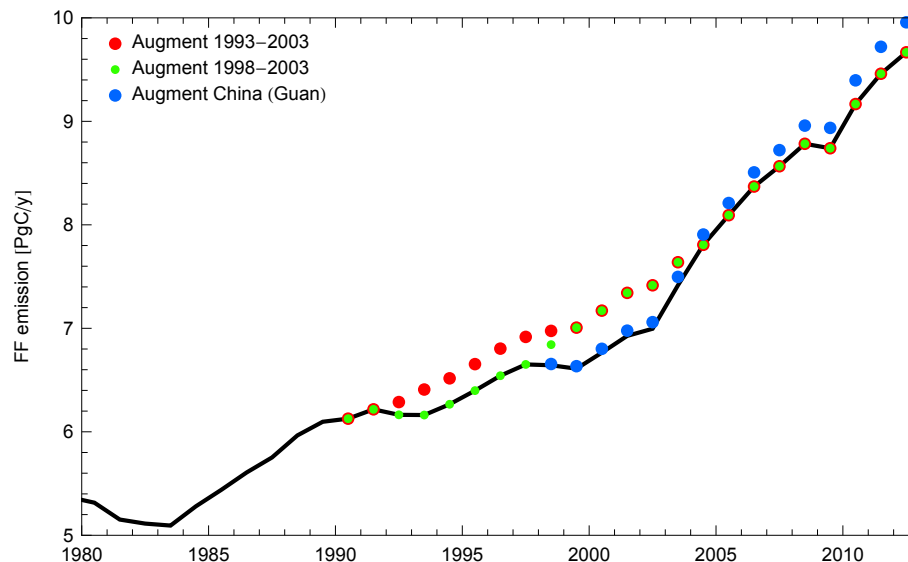


Fig. F1. Alternative trajectories for global CO₂ emissions from fossil fuels and other industrial sources (f_{FOSS}): (black) primary data; (red dots) f_{FOSS} augmented by 3 % from 1993 to 1998 and 6 % between 1999 and 2003 (with tapering); (green dots) f_{FOSS} augmented by 6 % between 1998 and 2003 (with tapering); (blue dots) f_{FOSS} if recent Chinese emissions are revised upward to use summed provincial rather than national data (Guan et al., 2012) (their Fig. 2). The trajectories shown by red and green dots follow suggestions of global emissions underestimates in the 1990s to early 2000s (Francey et al., 2010).

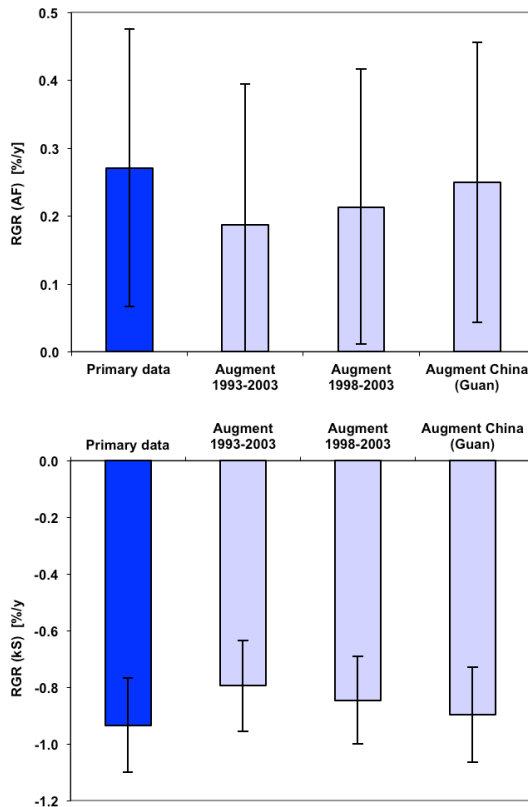


Fig. F2. Estimates of RGR(AF) (upper panel) and RGR(k_S) (lower panel), using primary data for f_{FOSS} (blue bars, as in Fig. 2) and three alternative f_{FOSS} trajectories shown in Fig. F1 (pale grey bars). Trends are estimated using Eq. (E2). All estimates are computed using data treatment (m, s, n) and the combined trend detection method, as for best estimates (Fig. 2 and Tables 1 and 2). Error bars show $\pm 1\sigma$ confidence intervals. For RGR(AF), all P values (probability of positive trend) exceed 0.69; for RGR(k_S), all P values (probability of negative trend) exceed 0.996.

Title Page

Abstract Introduction

Conclusions References

Tables Figures

◀ ▶

◀ ▶

Back Close

Full Screen / Esc

Printer-friendly Version

Interactive Discussion



The declining uptake rate of atmospheric CO₂ by land and ocean sinks

M. R. Raupach et al.

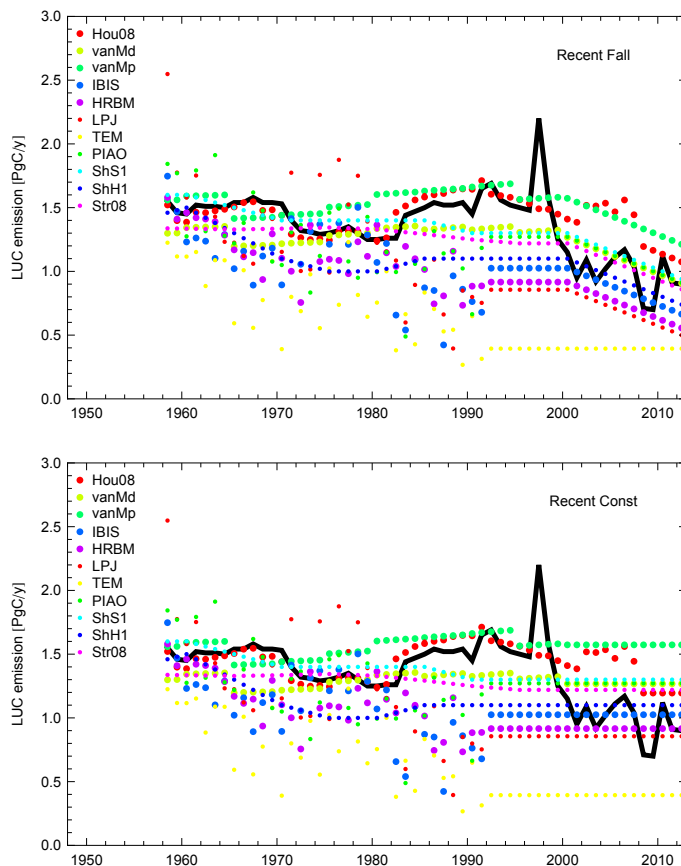


Fig. F3. Alternative trajectories for CO₂ emissions from net land use change (f_{LUC}): (black) primary data; (coloured dots) alternative trajectories described in Table F1. Upper and lower panels show “Recent Fall” and “Recent Const” extrapolations, respectively.

[Title Page](#)
[Abstract](#)
[Introduction](#)
[Conclusions](#)
[References](#)
[Tables](#)
[Figures](#)
[◀](#)
[▶](#)
[◀](#)
[▶](#)
[Back](#)
[Close](#)
[Full Screen / Esc](#)
[Printer-friendly Version](#)
[Interactive Discussion](#)

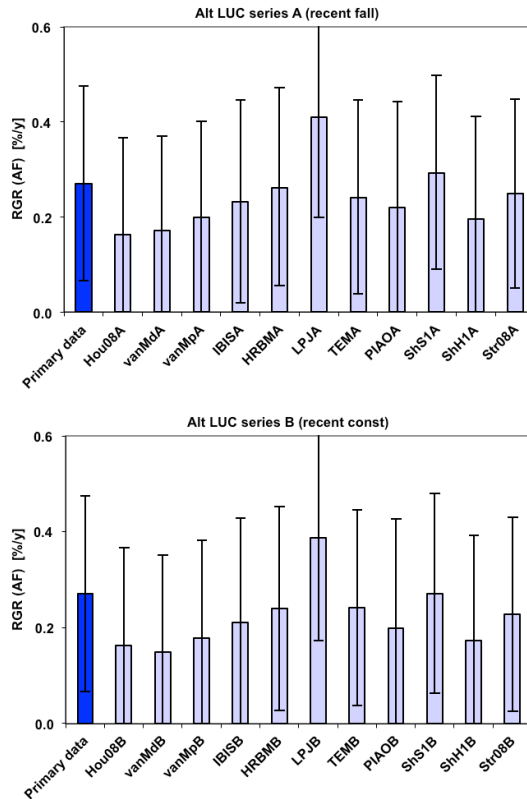


Fig. F4. Estimates of RGR(AF), using primary data for f_{LUC} (blue bars) and 11 alternative f_{LUC} trajectories (Table F1 and Fig. F3; pale grey bars). Trends are estimated using Eq. (E2). P values are shown in Table F1. All estimates are computed using data treatment (m, s, n) and the combined trend detection method, as for best estimates in Fig. 2 and Tables 1 and 2. Error bars show $\pm 1\sigma$ confidence intervals. Upper and lower panels show RGR(AF) using “Recent fall” and “Recent const” extrapolations, respectively.

The declining uptake rate of atmospheric CO₂ by land and ocean sinks

M. R. Raupach et al.

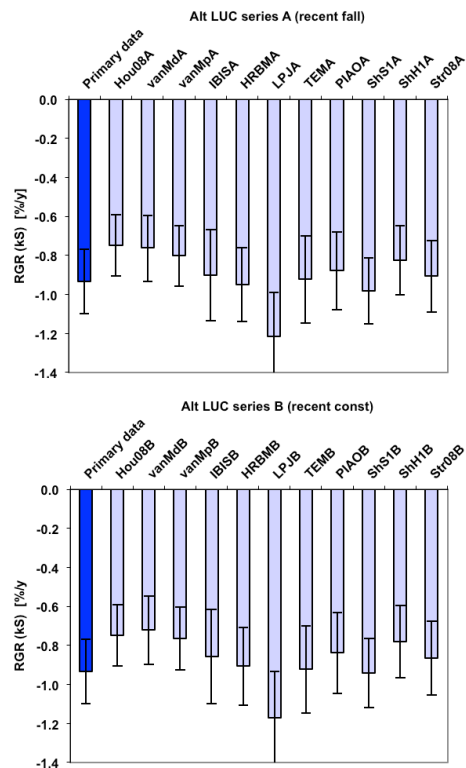


Fig. F5. Estimates of $RGR(k_S)$, using primary data for f_{LUC} (blue bars) and 11 alternative f_{LUC} trajectories (Table F1 and Fig. F3; pale grey bars). Trends are estimated using Eq. (E2). All P values (probability of negative k_S trend) exceeded 0.98 (values not tabulated). Other details follow Fig. F4.

The declining uptake rate of atmospheric CO₂ by land and ocean sinks

M. R. Raupach et al.

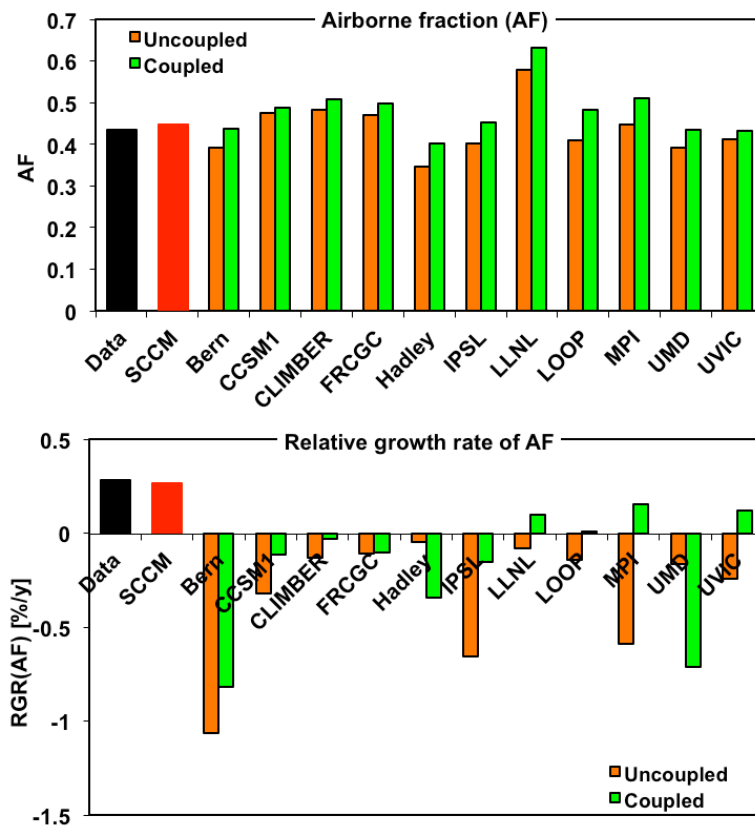


Fig. G1. Upper panel: mean AF over 1959.0–2013.0 from data (black bars), SCCM (Raupach, 2013) (red bars) and 11 C4MIP models (Friedlingstein et al., 2006) in both uncoupled and coupled modes (orange and green bars, respectively). Lower panel: relative growth rate RGR(AF), estimated using Eq. (E2).

The declining uptake rate of atmospheric CO₂ by land and ocean sinks

M. R. Raupach et al.

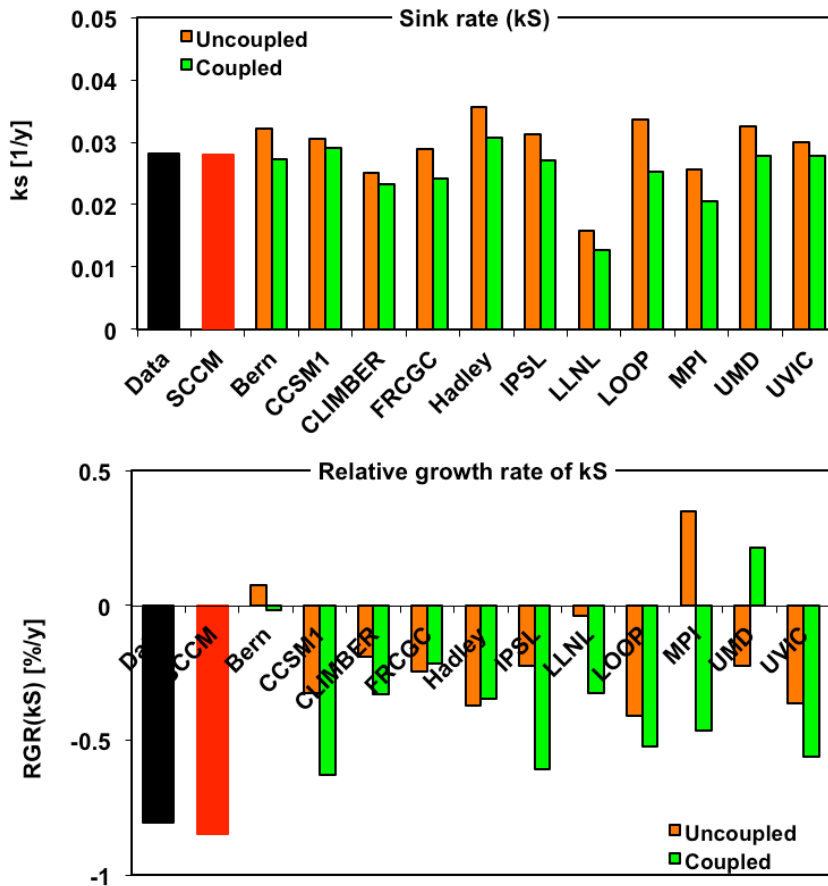


Fig. G2. Upper panel: mean sink rate k_S over 1959.0–2013.0 from data (black bars), SCCM (Raupach, 2013) (red bars) and 11 C4MIP models (Friedlingstein et al., 2006) in both uncoupled and coupled modes (orange and green bars, respectively). Lower panel: relative growth rate $RGR(k_S)$, estimated using Eq. (E2).